

(2)

2000 COPY

# NAVAL POSTGRADUATE SCHOOL

## Monterey, California

AD-A219 338



## THEESIS

DTIC  
REF ID: A67257  
RECEIVED  
19 MAR 1990  
C  
D  
E

OPTICAL EXCISOR MODELING

by

Daniel A. Marinsalta

September 1989

Thesis Advisor:

J. P. Powers

Approved for public release; distribution unlimited.

## UNCLASSIFIED

SECURITY CLASSIFICATION AUTOMATICALLY UPDATES

## REPORT DOCUMENTATION PAGE

1a REPORT SECURITY CLASSIFICATION UNCLASSIFIED	1b RESTRICTIVE MARKINGS		
2a SECURITY CLASSIFICATION AUTHORITY	3 DISTRIBUTION AVAILABILITY OF REPORT Approved for public release; distribution unlimited.		
2b DECLASSIFICATION/DOWNGRADING AUTHORITY			
4 PERFORMING ORGANIZATION REPORT NUMBER(S)	5 MONITORING ORGANIZATION REPORT NUMBER(S)		
6a NAME OF PERFORMING ORGANIZATION Naval Postgraduate School	6b OFFICE SYMBOL (If applicable)	7a NAME OF MONITORING ORGANIZATION Naval Postgraduate School	
6c ADDRESS (City, State, and ZIP Code) Monterey, CA 93943-5000	7b ADDRESS (City, State, and ZIP Code) Monterey, CA 93943-5000		
8a NAME OF FUNDING SPONSORING ORGANIZATION	8b OFFICE SYMBOL (If applicable)	9 PROCUREMENT INSTRUMENT IDENTIFICATION NUMBER	
9c ADDRESS (City, State, and ZIP Code)	10 SOURCE OF FUNDING NUMBERS		
	PROGRAM ELEMENT NO	PROJECT NO	TASK NO
	ACCRU UNIT ACCESSION NO		

11 TITLE (Include Security Classification)

OPTICAL EXCISOR MODELING, UNCLASSIFIED

12 PERSONAL AUTHORSHIP

Marinsalta, Daniel A.

13a TYPE OF REPORT Master's Thesis	13b TIME COVERED FROM 2/89 TO 9/89	14 DATE OF REPORT (Year, Month Day) September, 1989	15 PAGE COUNT 92
---------------------------------------	---------------------------------------	--	---------------------

16 SUPPLEMENTARY NOTATION The views expressed in this thesis are those of the author and do not reflect the official policy or position of the Department of Defense or the U.S. Government.

17 COSAT CODES	18 SUBJECT TERMS (Continue on reverse if necessary and identify by block number) Optical excisor - Bragg cell, - Acousto-optic, Spectrum Analyzer, - Excisor-detector. (F, )		
FIELD	GROUP	SUB GROUP	

19 ABSTRACT (Continue on reverse if necessary and identify by block number)

This work simulates an acousto-optic signal processing technique that can be used to filter radio-frequency (RF) electronic signals. Of particular interest is the removal or excision of narrowband interference from broadband signals. The program developed simulates the performance of a binary phase shift keying (BPSK) signal with a narrowband interference. The width and depth of notches that model an excisor-detector array are variable. In addition there is a capability to move the notches in order to place a notch over the interference for maximum filtering capability. A summary of several possible excisor techniques is presented.

20 DISTRIBUTION AVAILABILITY OF ABSTRACT <input checked="" type="checkbox"/> UNCLASSIFIED UNLIMITED <input type="checkbox"/> SAVE AS PPT <input type="checkbox"/> DTIC USERS	21 ABSTRACT SECURITY CLASSIFICATION UNCLASSIFIED
22a NAME OF RESPONSIBLE INDIVIDUAL JOHN P. POWERS	22b TELEPHONE (Include Area Code) (408) 646-2081
22c OFFICE SYMBOL 62	

Approved for public release; distribution unlimited.

Optical Excisor Modeling

by

Daniel Alberto Marinsalta  
Lieutenant, Argentine Navy  
Escuela Naval Militar, Argentina, 1976

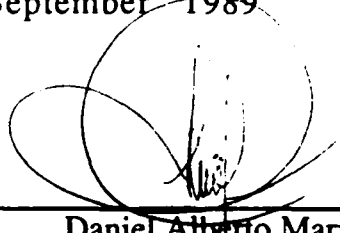
Submitted in partial fulfillment of the  
requirements for the degree of

MASTER OF SCIENCE IN SYSTEM ENGINEERING  
(ELECTRONIC WARFARE)

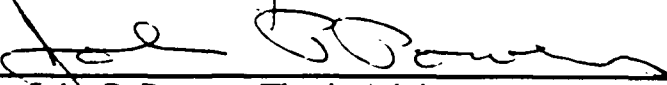
from

NAVAL POSTGRADUATE SCHOOL  
September 1989

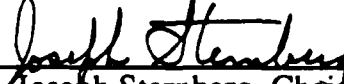
Author:

  
Daniel Alberto Marinsalta

Approved By:

  
John P. Powers, Thesis Advisor

  
David D. Cleary, Second Reader

  
Joseph Sternberg, Chairman,  
Electronic Warfare Academic Group

## ABSTRACT

This work simulates an acousto-optic signal processing technique that can be used to filter radio-frequency (RF) electronic signals. Of particular interest is the removal or excision of narrowband interference from broadband signals. The program developed simulates the performance of a binary phase shift keying (BPSK) signal with a narrowband interference. The width and depth of notches that model an excisor-detector array are variable. In addition there is a capability to move the notches in order to place a notch over the interference for maximum filtering capability. A summary of several possible excisor techniques is presented.

Accession No.	
NTIS Title	
DTIC Title	
Unclassified	
Justification	
By _____	
Distribution/	
Availability Code	
Dist	Avail and/or Special
A-1	



## **DISCLAIMER**

The reader is cautioned that computer programs developed in this research may not have been exercised for all cases of interest. While every effort has been made, within the time available, to ensure that the programs are free of computational and logic errors, they cannot be considered validated. Any application of these program without additional verification is at the risk of the user.

## TABLE OF CONTENTS

I.	INTRODUCTION .....	1
A -	BACKGROUND.....	1
B -	OPTICAL EXCISION.....	4
C -	THESIS OBJECTIVE.....	8
II.	GENERAL DESCRIPTION OF THE SYSTEM.....	9
III.	THE MATHEMATICAL MODEL.....	14
IV.	COMPUTER PROGRAM DESCRIPTION.....	19
A -	INTRODUCTION .....	19
B -	PROGRAM STRUCTURE.....	20
C -	THE PROGRAM.....	21
1 -	BLOCK INP_B.m.....	22
2 -	BLOCK M_BPSK.m.....	22
3 -	BLOCK FILTER.m.....	22
4 -	BLOCK S_BPSK.m .....	26
5 -	BLOCK FFT_B.m.....	30
6 -	BLOCK S_FIL.m.....	33
7 -	BLOCK IFFT_B.m.....	36
8 -	BLOCK COD_B.m.....	37
V.	PROGRAM EVALUATION .....	41
A -	TEST N° 1 .....	41
B -	TEST N° 2 .....	45
C -	TEST N° 3 .....	49
D -	TEST N° 4 .....	52

E- OTHER TESTS.....	55
1 - NO-FILTER TEST .....	55
2 - MOVING THE EXCISOR-DETECTOR .....	56
VI. CONCLUSIONS AND RECOMMENDATIONS.....	61
APPENDIX A - NOTATION USED IN THE PROGRAM.....	62
APPENDIX B - COMPUTER PROGRAM .....	64
BLOCK Input initial Data (INP_B.m).....	64
BLOCK Main Control (M_BPSK.m).....	65
BLOCK Detector Array Filter Signal (FILTER.m) .....	66
BLOCK BPSK Signal Generator (S_BPSK.m).....	67
BLOCK FFT of BPSK Signal (FFT_B.m) .....	69
BLOCK Signal Filtering on the Detector Array (S_FIL.m).....	70
BLOCK IFFT Signal Filtered (IFFT_B.m).....	71
BLOCK Coherent Detector (COD_B.m) .....	72
APPENDIX C - INFORMATION ABOUT NOTCHES .....	74
APPENDIX D - DEFINITIONS.....	77
LIST OF REFERENCES.....	79
INITIAL DISTRIBUTION LIST .....	81

## LIST OF FIGURES

<b>Figure 1</b>	- Acousto-optic spectrum analyzer.....	1
<b>Figure 2</b>	- Optical excisor architecture .....	3
<b>Figure 3</b>	- Optical excisor characteristic.....	4
<b>Figure 4</b>	- Bragg diffraction in a spectrum analyzer.....	9
<b>Figure 5</b>	- Optical excisor.....	12
<b>Figure 6</b>	- System representation.....	18
<b>Figure 7</b>	- Program structure.....	21
<b>Figure 8</b>	- Excisor-detector array .....	24
<b>Figure 9</b>	- Filter magnitude response .....	25
<b>Figure 10</b>	- Binary random data.....	28
<b>Figure 11</b>	- BPSK signal and modulated waveform.....	30
<b>Figure 12</b>	- BPSK signal plus interference.....	31
<b>Figure 13</b>	- PSD of a test BPSK signal plus interference.....	33
<b>Figure 14</b>	- Theoretical and calculated PSD of a BPSK signal .....	33
<b>Figure 15</b>	- Filter transfer function and test signal spectrum.....	34
<b>Figure 16</b>	- Filtered and original signal spectrum comparison.....	35
<b>Figure 17</b>	- Original and recovered BPSK signal .....	36
<b>Figure 18</b>	- Coherent detection.....	37
<b>Figure 19</b>	- Integrate and dump detector .....	38
<b>Figure 20</b>	- Integrator output ( $T_b = 0.78 \mu\text{sec}$ ).....	38
<b>Figure 21</b>	- Original and recovered binary data.....	39
<b>Figure 22</b>	- Error detection.....	39
<b>Figure 23</b>	- Output Test N° 1 .....	45

Figure 24 - Output Test Nº 2.....	4 8
Figure 25 - Output Test Nº 3.....	5 1
Figure 26 - Output Test Nº 4.....	5 4
Figure 27 - Original and recovered BPSK signal .....	5 5
Figure 28 - Original and recovered binary data.....	5 6
Figure 29 - Error detection output.....	5 6
Figure 30 - Test signal spectrum (notch at 67.35 MHz).....	5 7
Figure 31 - Test signal spectrum (notch at 67.38 MHz).....	5 7
Figure 32 - Test signal spectrum (notch at 67.39 MHz).....	5 8
Figure 33 - Test signal spectrum (notch at 67.40 MHz).....	5 8
Figure 34 - Test signal spectrum (notch at 67.41 MHz).....	5 9
Figure 35 - Test signal spectrum (notch at 67.42 MHz).....	5 9

## **ACKNOWLEDGEMENTS**

In appreciation for their time, effort, and patience, many thanks go to my superiors, instructors, and fellow students. Also, to those who made this tour possible, I extend my heartfelt gratitude for this outstanding experience at the Naval Postgraduate School. A special mention goes to my Advisor, Dr. John P. Powers; thank you for your insight, extreme patience and the chance to learn from your experience. But most off all, this work could not have been completed without the love, understanding, and unselfish devotion of my friend and partner in life. Thank you, Mónica.

## I. INTRODUCTION

### A - BACKGROUND

Many companies are designing, developing, and field-testing Acousto-optics Spectrum Analyzers (AOSA) for communications, radar and electronic warfare surveillance. In many such applications, acousto-optics is not merely a good choice—it is the only choice. [Ref. 1]

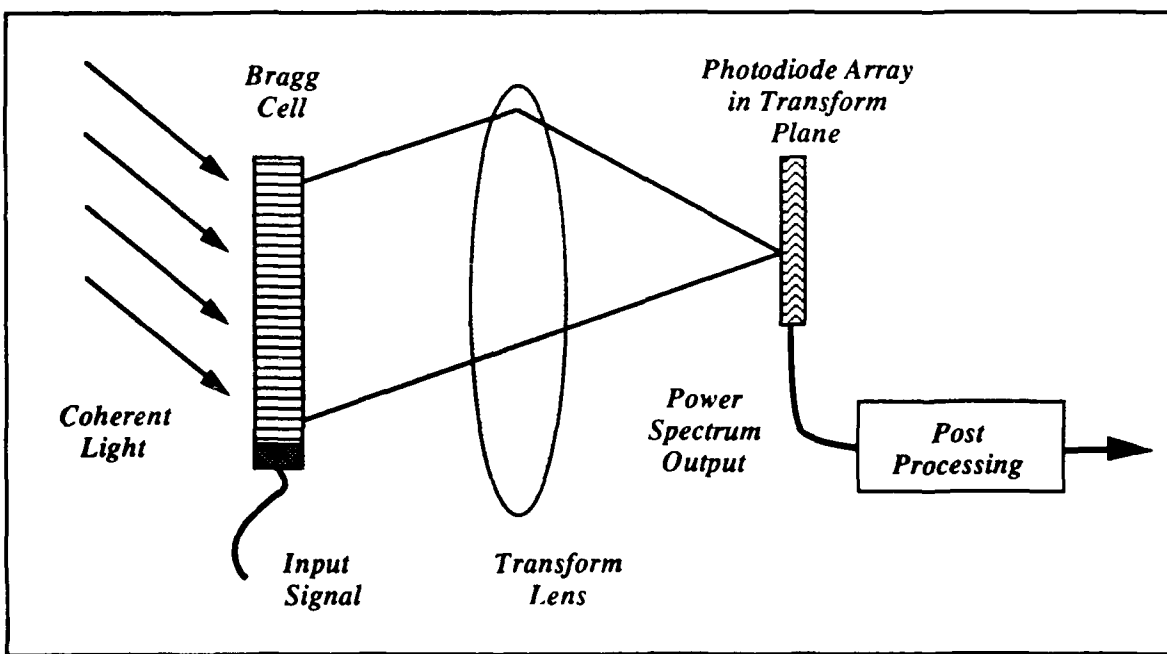


Figure 1 - Acousto-optic spectrum analyzer

As an introduction to acousto-optic spectrum analyzers consider the system in Figure 1. Coherent light illuminates a one dimensional

spatial light modulator, in this case a Bragg cell. The light diffracted by the cell is collected by the lens and focused onto a photodiode array. The light amplitude at the photodetector is the spectrum of the information in the Bragg cell. This serves to illustrate the simplicity of one optical technique for calculating spectra. [Ref. 2]

The problem of rejecting relatively narrowband interference signals is becoming more important as the bandwidth of digital communications systems increases. Acousto-optics is showing promise in this area [Ref. 1]. An optical implementation of this technique is shown in Figure 2.

In order to implement an optical excisor we need more elements interacting in the AOSA basic architecture than was presented in Figure 1. As showed in Figure 2, the signal  $s(t)$  is applied to a Bragg cell (1). The cell is illuminated with coherent light (2) and the spectrum of the signal is formed on the photodetector array (3). The light at each photodetector has an amplitude proportional to the amplitude of the corresponding acoustic frequency in the Bragg cell. A given acoustic frequency component acts as a moving diffraction grating; for this reason the light diffracted by it is Doppler frequency-shifted by the frequency of the acoustic signal. The acoustic signal component can be reconstructed by down-converting the diffracted light to the acoustic frequency. This is achieved by adding the optical signal to a reference beam (4). The resulting combined beams fall on a photodetector array. The photodetector

produces an electrical signal with a frequency equal to the difference between the frequencies of the two optical inputs. This results in the recovery of the acoustic frequency components and hence the recovery of the input radio frequency component.

The optical excisor continuously forms the spectrum of a broadband electrical signal and reconstructs an exact replica of the input signal from that spectrum. The important feature of this process is that the spectrum is spatially distributed and is physically available at the detector plane for removing an undesired portion of the spectrum. For example, the excision of narrowband interference from broadband signals is possible.

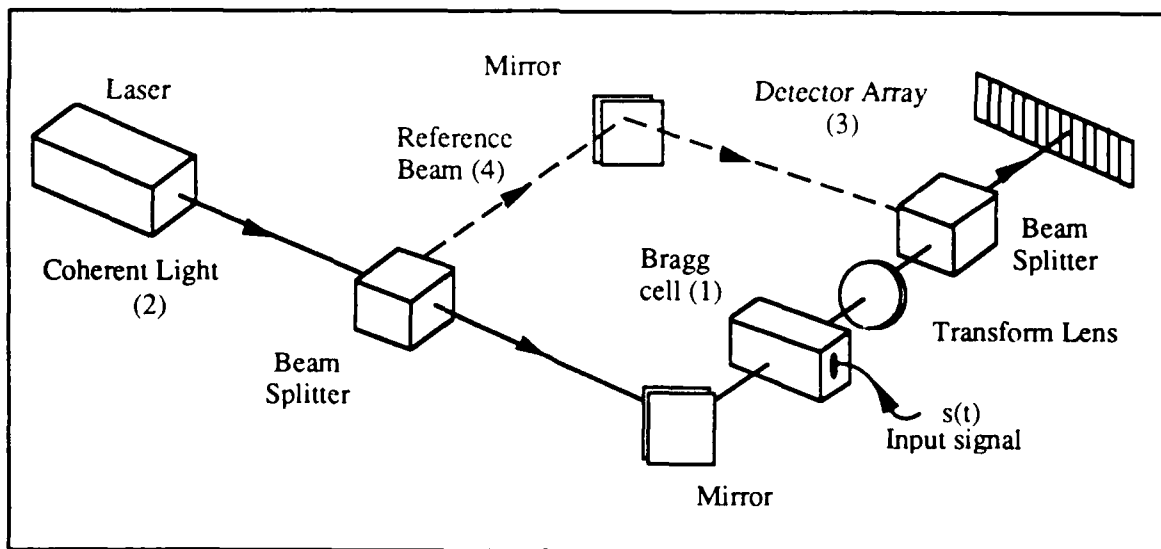


Figure 2 - Optical excisor architecture

Two significant characteristics of an optical excisor are: 1) it has an RF signal input and an RF signal output, 2) it is a predetection signal processor producing a continuous coherent output [Ref. 3].

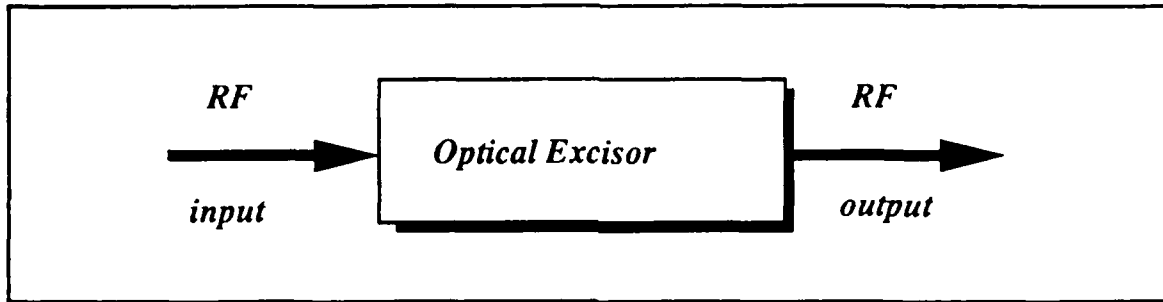


Figure 3 - Optical excisor characteristic

## B - OPTICAL EXCISION

If we have two input signals that are sufficiently different in frequency to be resolved in the back focal plane, a spatial light modulator can be placed in this location and used to turn off either one or both of the input signals [Ref. 3].

Another technique would be to block the light of one signal by using an aperture or small wire in the focal plane, thereby allowing passage of only the desired signal. [Ref. 3]

A broadband signal that has a narrowband interference signal in its spectrum can be applied to the input of the optical excisor. The narrowband signal will form a small spot of light, while the broadband signal will extend over a relatively large area. Using a small wire, the strength of the interference can be significantly reduced while only blocking a small portion of the broadband signal. The bigger the wire, the more the interference will be blocked, and

therefore the more it will be attenuated at the output. However, a large wire will also remove more of the broadband output signal and perhaps begin to cause significant degradation in the broadband output waveform. The task for the designer of an optical excisor is to optimize the transfer function to achieve a useful amount of attenuation of the narrowband interference without removing significant portions of the broadband signal. [Ref. 3]

An alternative excision approach is to place a material such as photochromic glass or photodichroic crystal in the focal plane. These materials will darken in an amount proportional to the irradiance of the incident light (much like photographic film, but in real time). Narrowband interference signals, because of their relatively high intensity, will be attenuated automatically [Ref. 3].

As can be seen, using different excision methods in the optical Fourier transform plane will create excision notches with different properties.

The following is a summary of the different experiments found in references which illustrate various techniques for excision as well as their results.

*Thin opaque wires* of known diameters placed in the transform plane can create narrow excision notches. Using thin bare copper wire in the transform plane, it blocks a portion of the diffracted signal spectrum, thereby creating an excision notch. In different experiments it was found that the attenuation achieved was about 40 dB with inexpensive lenses. [Ref. 6]

*A Pockel's Readout Optical Modulator* (PROM) spatial light modulator can be used in a fashion which automatically attenuates narrowband interferences. The PROM has nonlinear clipping characteristics which attenuates intense signals, while weaker signals pass unaffected. In fact, a strong signal can be attenuated below the level of a weak signal. Broadband signals should be relatively unattenuated compared to more powerful narrowband signals because their power spectrum distribution in the optical Fourier transform plane will be below the clipping threshold of the PROM.

The PROM optical clipper is intended to be utilized as an image storage device which is written with blue light and read out with red light. The experiment reported in reference 3 utilized the red HeNe laser light for both writing and reading functions. A strong narrowband interference signal will create a bright red spot in the transform plane which effectively acts to write a *dark spot* on the PROM. This dark spot prevents the narrowband interference from being passed to the photodetector. Thus the strong narrowband interference signal effectively attenuates itself. [Ref. 3]

Reference 3 showed that the PROM-based excisor has attenuated a narrowband signal by 28 dB relative to the broadband pulsed signal. It demonstrated encouraging results, but the utility in a practical system is limited by the fact that a PROM is an image storage device which must be cycled through an erase phase followed by a read/write phase.

Variations of the PROM are being considered which will avoid the image storage properties of the current PROM so that time-framing and cycling problems may be avoided. [Ref. 3]

A *Programmable lead lanthanum zirconate* (PLZT) ceramic modulator can also be used in the transform plane. A programmable PLZT ceramic light modulator will allow the filter magnitude response to be controlled by electronic means. By applying a transverse electric field to the PLZT ceramic, the polarization of the transmitted optical beam can be rotated. By placing the PLZT ceramic between crossed optical polarizers, the intensity of the transmitted optical beam can be electronically controlled. Spatial control of the transmitted optical intensity can be obtained by having separately addressable electrodes across the aperture of the PLZT ceramic. [Ref. 3]

The results of the PLZT-based optical excisor showed that 18 dB of excision could be obtained while an opaque wire having a similar notch width obtained 23 dB of excision depth. [Ref. 3]

Another form of excision is due to the spaces between detectors in a detector array to perform the optical excision. In the frequency domain, they are represented by a set of notches that are periodically spaced. The width of the notches is proportional to the spaces between the detector elements. The depth depends on the width and the diffraction effects (A similar model also applies when a linear array of fiber optic cables leading to individual detectors is used to measured the light properties). It is this latter form of excision that we wanted to study.

## C. THESIS OBJECTIVE

The objective of the research described in this thesis was to develop a computer program which, through simulation, would provide a capability to evaluate the filtering ability of gaps between detectors in a detector array versus narrowband interference in a broadband signal.

Using the Naval Postgraduate School's library and computer facilities, we wanted to develop a computer program based in MATLAB386 [Ref. 4] using a Compaq 386/20 computer.

The specific goals were to evaluate the distortion on the original signal due to the filtering process and to examine the notch dimensions (width and depth) for their effect on the filtering capability.

Chapter 2 serves as a brief description of the optical excisor system. This chapter describes an acousto-optic signal processing technique that can be used to filter radio-frequency electronic signals. A discussion of the mathematical model chosen for the simulation is given in Chapter 3. The detailed description of the computer program is presented in Chapter 4, showing the information available during the simulation. Chapter 5 contains the simulation results and an evaluation of the program, and finally Chapter 6 contains concluding remarks and suggests areas of future research.

## II. GENERAL DESCRIPTION OF THE SYSTEM

The optical excisor separates the input signal  $s(t)$  into each of its Fourier components, processes the magnitude and phase of each Fourier component and finally sums the modified Fourier components into a filtered signal. A general description of an optical excisor can be based on the architecture shown in Figure 5.

The electrical input signal  $s(t)$  typically is derived from a broadband antenna, downconverter, and amplifiers. This signal is applied to a Bragg cell illuminated by a coherent light, illustrated in Figure 4.

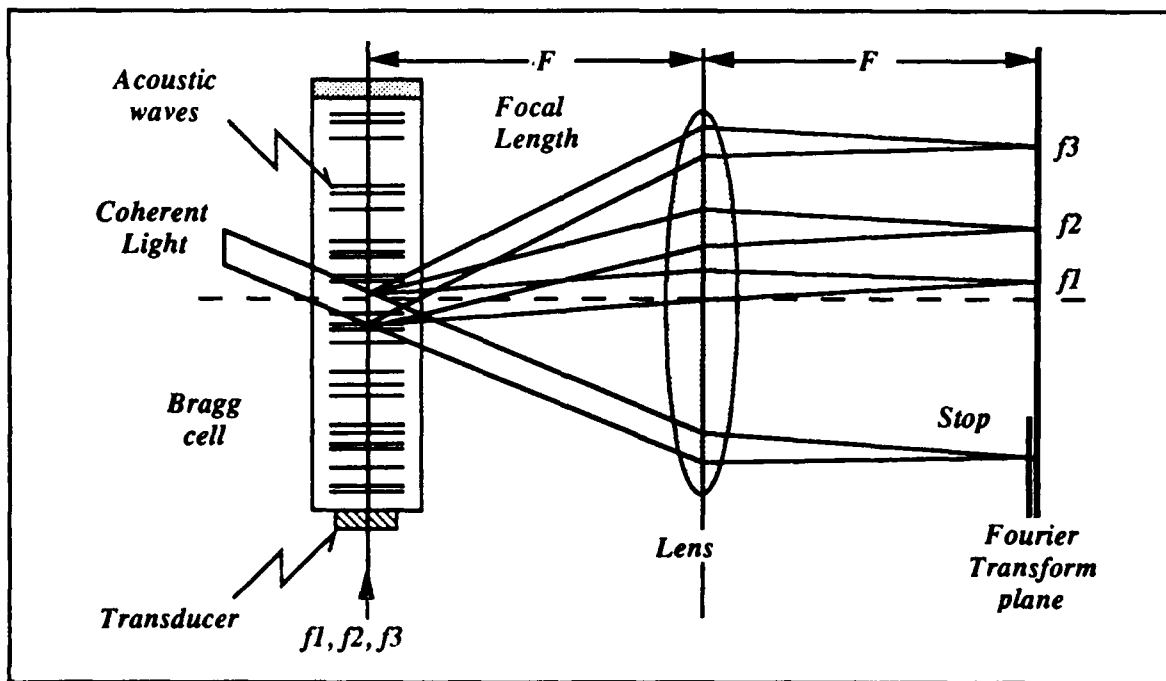


Figure 4 - Bragg diffraction in a spectrum analyzer

The acousto-optic modulator is a block of transparent material with a piezoelectric transducer bonded to one end. The other end is tapered to trap the acoustic waves and loaded to provide an effective acoustic termination. A piezoelectric transducer is sandwiched between electrodes and vibrates in synchronism with the applied voltage. When driven by an electrical signal, the transducer excites an acoustic which is a replica of that signal. This acoustic wave propagates down the long axis of the Bragg cell and produces compressions and rarefractions in the material [Ref. 2]. The interaction between coherent light and the acoustic wave results from an increase in the index of refraction of the material at a compression and a decrease in the index at a rarefaction. This results in a modulation in phase of the light passing through the acousto-optic modulator. The resulting spatial phase distribution can be considered equivalent to a superposition of plane waves of various phases and amplitudes. By using a lens to focus the various diffracted plane waves, each wave can be separated and the amplitude and phase of each spectral component of the original input signal can be measured. So far the description is similar to an AOSA [Ref. 3].

In addition to diffracting the plane waves based on the spectrum of the input signal, the acousto-optic modulator also Doppler shifts the diffracted plane waves. The amount of Doppler shift is exactly equal to the frequency of the input signal, and therefore, if the

amount of Doppler shift is measured, the frequency of the input can be determined. [Ref. 3]

An easy way for measuring an optical Doppler shift is to add some unshifted light from the optical source and process the summed signal electronically. The resulting beat signal frequency will be equal to the frequency difference between the two signals and hence be equal to the amount of Doppler shift. [Ref. 3]

The unshifted reference beam, in Figure 5, is derived from the spatially coherent optical source using optical splitters (partially reflecting mirror). The light reflected by this beam splitter is set to mirror 1 which then reflects the light to the acousto-optic modulator. The light transmitted by the beam splitter is reflected by mirror 2 up to a second beam splitter, reflecting some of the reference beam to the photodetector array. The second beam splitter also passes some of the light diffracted by the acousto-optic modulator. By adjusting the mirrors and beam splitters, both the reference beam and the diffracted beam appear to come from the same direction and are added together by the beam splitter before the detector array. By using a spatial light modulator in the transform plane and selectively passing only the desired portions of the spectrum, interference signals can be rejected [Ref. 3]. The photomixing and signal summing by the detector reconstructs the time domain waveform of the desired portion of the input signal and provides a coherent continuous output  $i(t)$ .

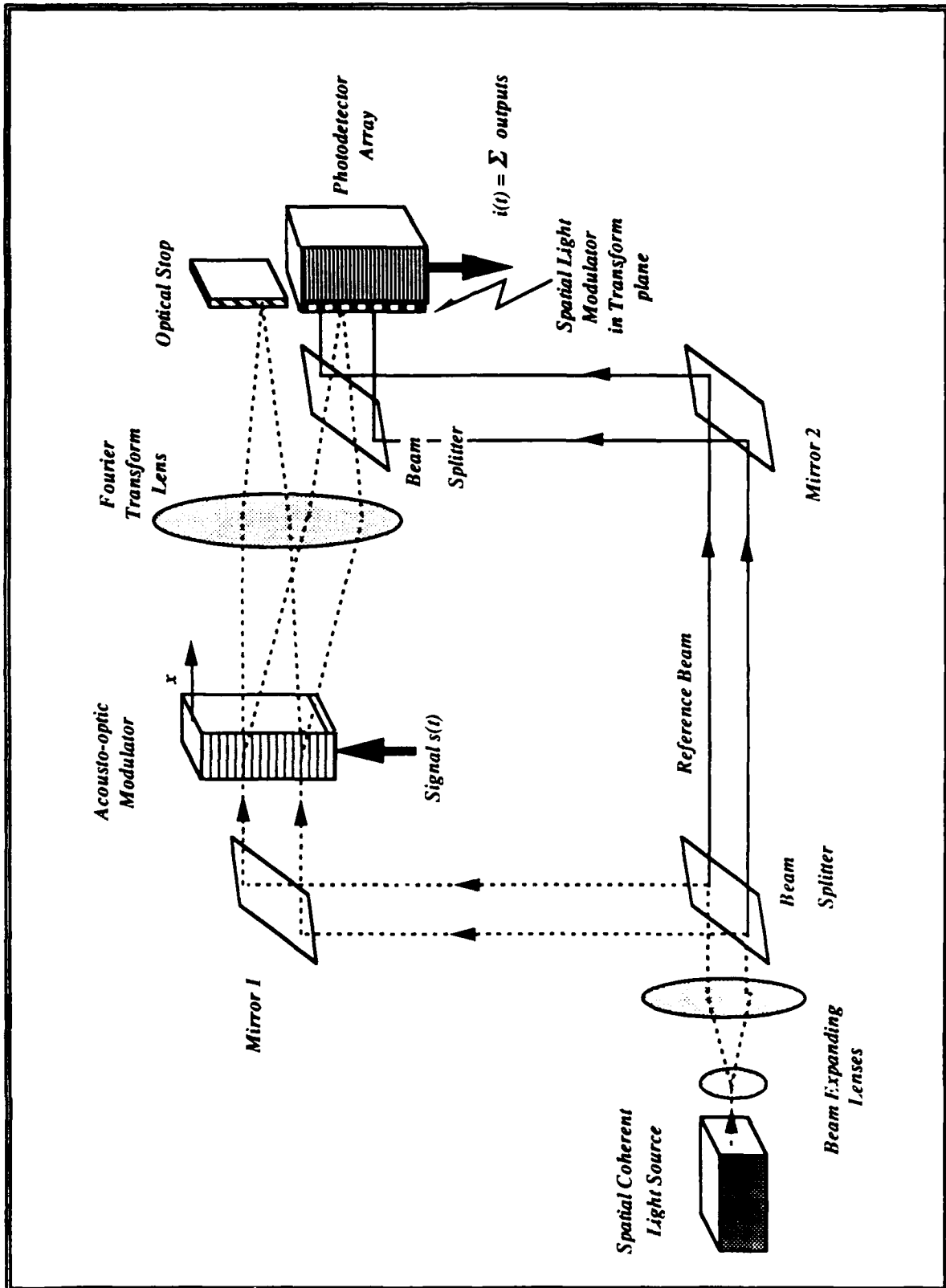


Figure 5 - Optical excisor

The five main components of the system presented are:

- (1) spatial coherent light source;
- (2) one-dimensional, acousto-optic modulator;
- (3) lens for Fourier transformation;
- (4) a frequency plane spatial modulator, and
- (5) the photodetector array.

The present work considers the detector array acting as a spatial light modulator in the frequency plane; for this reason, from now on, it will be called as "excisor-detector" array. This technique is of particular importance in rejecting narrowband interference in wideband communications systems. By using the spaces between detectors as notches in the frequency domain, one can control the frequency rejection to match the signal environment. The signal environment may consist of a wideband signal with a narrowband interference signal located at some arbitrary frequency within the bandwidth of the desired wideband signal. The object is to block the narrowband interference signal with one of the narrow bandwidth frequency rejection notches of the excisor-detector array.

### III. THE MATHEMATICAL MODEL

A more precise description of the operation in the optical excisor can now be given. The broadband signal including a narrowband interfering signal is  $s(t)$ . The collimated coherent input light is diffracted through an angle proportional to the acoustic frequency present in the Bragg cell. This acoustic frequency results from the applied electrical signal  $s(t)$ , where  $s(t)$  is real. The diffracted optical signal amplitude at the exit port of the cell is proportional to  $s(t-x/v)$ , where  $x$  is the distance from the input transducer and  $v$  the acoustic velocity. The acousto-optic (AO) cell has a finite aperture equal to  $T$ , where  $T$  is the transit time of the acoustic wave in the AO cell. This finite aperture corresponds to an apodization of the acoustic signal such that the signal may now be represented by  $s(t-x/v-T/2)$  [Ref. 2]. Also for this analysis, the AO cell is assumed to operate over an octave RF bandwidth (or less) and the positive first order diffraction is used [Refs. 2, 3 and 5].

The optical system takes the Fourier transform with respect to the spatial variable  $x$ .

$$S(p, t) = \int_{-L/2}^{+L/2} s\left(t - \frac{x}{v} - \frac{T}{2}\right) e^{-jpx} dx \quad (1)$$

where  $L$  is equal to the length of the AO cell and  $p$  is the spatial

frequency variable. Associated with each spatial frequency  $p$  is a temporal frequency  $\omega = pv$ .

A change of variables (where  $u=t-x/v-T/2$ ) yields:

$$S(p, t) = v e^{-j(t - \frac{T}{2})pv} \int_t^{t - T} s(u) e^{jpv u} du \quad (2)$$

$$S(pv) = \int_t^{t - T} s(u) e^{jpv u} du \quad (3)$$

Equation (2) is seen to be the Fourier transform of the portion of  $s(t)$  within the aperture of the Bragg cell. The exponential phase term indicates that the light diffracted to position  $p$  is frequency shifted by an amount equal to the temporal frequency  $\omega$ .

The detectors respond to light intensity rather than light amplitude, for this reason it is necessary to bring in a reference wave intersecting the frequency plane. The reference wave has a flat wavefront which may be parallel with the frequency plane or intersect the frequency plane at a small angle  $\phi$ . This reference wave with tilt angle  $\phi$  may be written as  $Ae^{j\phi p}$ , where  $A$  is the amplitude of the reference wave [Ref. 5].

The total amplitude in the output plane,  $T(p,t)$ , is the sum of the reference wave and the transform of the signal multiplied by the filter signal,  $H(p,t)$ , (representing the spaces between detectors).

$$T(p, t) = [Ae^{j\phi p} + v e^{-jpv(t - \frac{T}{2})} S(pv)] \times H(p, t) \quad (4)$$

The corresponding intensity distribution is:

$$I_o(p, t) = |T(p, t)|^2 \quad (5)$$

$$\begin{aligned} |T(p, t)|^2 &= H(p, t)^2 A^2 + v^2 S(pv)^2 H(p, t)^2 \\ &\quad + 2 \operatorname{Re}[S(pv)^2 H(p, t)^2 e^{jp(\phi + v(t - \frac{T}{2}))}] \end{aligned} \quad (6)$$

where  $\operatorname{Re}(x)$  means the real part of  $(x)$ . The output from the excisor-detector array is the summation of all photodiodes; this corresponds to an integration over the spatial variable  $p$ .

$$\int I_o(p, t) dp = \int |T(p, t)|^2 dp \quad (7)$$

$$\begin{aligned} &= \int \left| H(p, t) v e^{-jv(t - \frac{T}{2})} S(pv) + 2A e^{j\phi} p H(p, t) \right|^2 dp \\ &= \int v^2 S(pv)^2 H(p, t) dp + A^2 \int H(p, t)^2 dp \\ &\quad + 2 A v \operatorname{Re} \int H(p, t) S(pv) e^{jp(\phi + v(t - \frac{T}{2}))} dp \end{aligned} \quad (8)$$

As stated before, the  $s(t)$  signal is assumed to be real and to occupy an octave or less of bandwidth. Under these assumptions the first two terms of equation (8) do not contribute in-band frequency components to the reconstruction of the original input signal [Refs. 2 and 5].

The last term of equation (8) represents an inverse Fourier transform of the original Fourier transformed signal, which yields the original signal with time delay equal to half the time aperture of the AO cell plus the delay equal to the reference beam.

$$\begin{aligned} & 2 A v \operatorname{Re} \int H(p,t) S(p,v) e^{jp(\frac{\phi}{v} + (t - \frac{T}{2}))} dp = \\ & = 2 A h(t) s(t - \frac{T}{2} + \frac{\phi}{v}) \end{aligned} \quad (9)$$

Equation (9) represents the filtered reconstruction of the original signal.

The mathematical model described can be summarized in Figure 6 for the program calculations. The test BPSK signal  $V_i(t)$  is injected in the input. The quantity  $V_i(f)$  represents the FFT of the input signal,  $H(f)$  is the transfer function of the detector-excisor array, and  $V_o(f)$  represents the filtered signal. Recovering the filtered signal back to the time domain, the IFFT is performed to obtain  $V_{ir}(t)$  which is electronically processed to detect the original binary information.

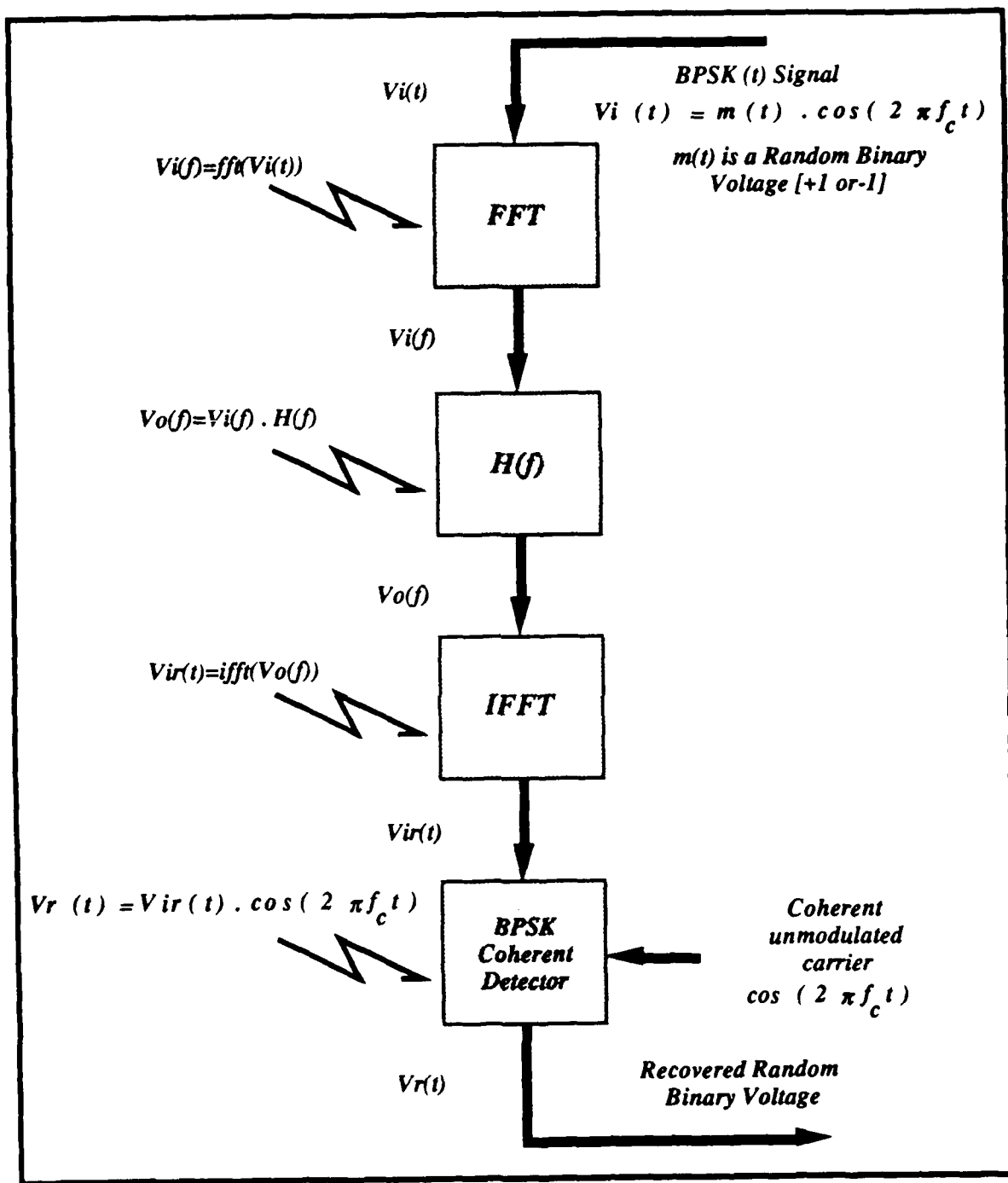


Figure 6 - System representation

## IV. COMPUTER PROGRAM DESCRIPTION

### A - INTRODUCTION

The purpose of the simulation program is to model and analyze the effects of an optical excisor. Of particular interest is the removal of narrowband interference from a BPSK communication signal. This interference is removed using the notches between detectors, in a detector array, as a filter.

Optical excisor performance is measured in terms of how well the offending signal frequency components are removed from the output, and how much of the original signal of interest is corrupted through loss of frequency components during the filtering process. [Ref. 6]

The excisor-detector array contains gaps between detectors that appear as notches in the frequency domain (filter). For our purpose the width and depth of the notches can be varied to simulate optical and mechanical adjustments and the effects produced on the test signal can be observed.

The modeling is intended to be simple enough as not to obscure the fundamental ideas but complete enough to include important effects and avoid incorrect conclusions.

## B- PROGRAM STRUCTURE

The program was divided into eight different blocks that represent various stages in the process. Each of these blocks performs specific functions presented in Table I.

A simplified diagram of the program is presented in Figure 7 which gives the general structure of the system.

TABLE I - BLOCK FUNCTIONS

BLOCKS	FUNCTIONS
• INP_B.m	1- Lets you input the data for the simulation.
• M_BPSK.m	1- Master Block executes other sections. 2- Controls the loops to simulate the movement of the Excisor-detector array.
• FILTER.m	1- Builds the filter. 2- Generates the frequency axis.
• S_BPSK.m	1- Creates the BPSK signal. 2- Creates the interference. 3- Generates the random numbers. 4- Generates the time axis.
• FFT_B.m	1- Calculates the FFT of the input test signal. 2- Calculates the FFT Theoretical for comparison.
• S_FIL.m	1- Computing the filtering process in the frequency domain.
• IFFT_B.m	1- Calculates the IFFT of the filtered signal.
• COD_B.m	1- Coherent detection of the filtered signal.

## C- THE PROGRAM

In this section a detailed explanation of each block is presented for a better understanding of how the computer program works.

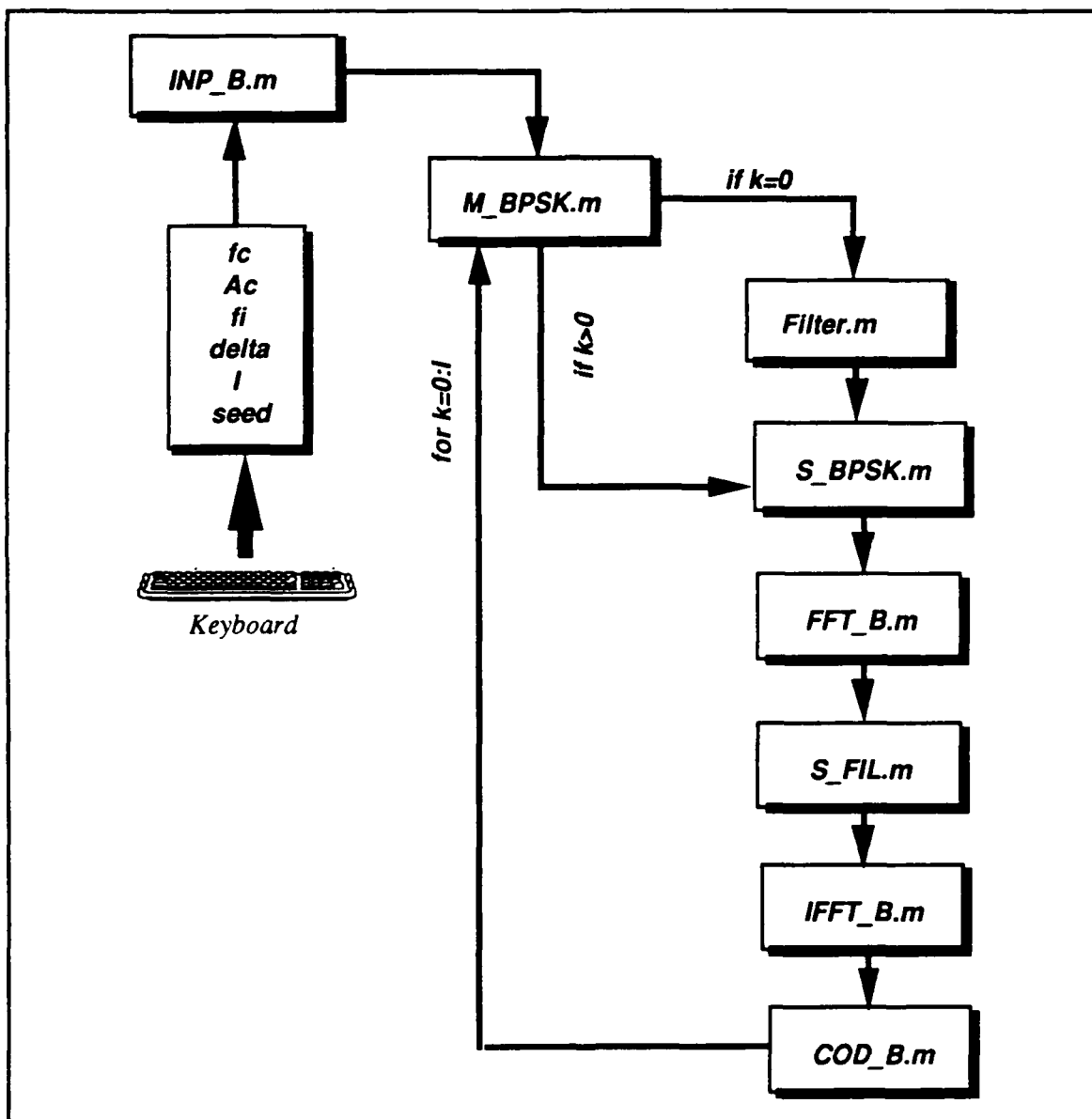


Figure 7 - Program structure

### **1 - BLOCK INP\_B.m**

The input data block is for introducing the variables needed to run the program like the carrier frequency (fc), the amplitude of the signal (Ac), the central frequency of the interference signal (fi), the step interval in order to simulate the movement of the detector array (delta), the number of loops that is needed for the program (I), and the seed number for the random number generator (seed). All values are presented on the screen.

### **2 - BLOCK M\_BPSK.m**

This block controls the sequence during the simulation and the loop to simulate the movement of the excisor-detector array. In order to reduce the amount of memory, the data is stored in temporarily files to be used by the other section. After each block has been run and the data has been stored in a temporary file, the memory is cleared before executing the next block to keep the computer from running out of memory.

### **3 - BLOCK FILTER.m**

The main functions of the Filter.m block are to build the filter transfer function and to create the frequency axis that will be used by the simulation. The filter consists of a signal that represents a

detector array in the frequency domain. An ideal representation of the excisor-detector array is showed in Figure 8. In Figure 9, the filter magnitude response of the model of the excisor-detector array is presented. The width (w) may vary from 0 to 120 KHz and the depth (d) from 0 to -90 dB. Figure 8 also shows the center frequency for each notch in the excisor-detector array assuming that the array is centered at 70 MHz. Appendix C provides useful information to work with the filter, like the frequency at which any notch starts and ends for a given width and the correct value of notch depth that represents the desired attenuation.

Performing this RF filtering process in the frequency plane of an optical spectrum analyzer has advantages over the electronic techniques [Ref. 6]. When an object is placed in the frequency plane of the optical spectrum analyzer, the magnitude of the affected frequency interval is attenuated and the phase remains constant. Also, many filters may be realized simply by varying the size of the notch in the frequency plane.

The excisor-detector is placed at one focal length away from the Fourier transform lens into the frequency plane. It has 13 photodiodes elements that represent the different channels 750 KHz wide, adding to a total 9.75 MHz window as shown in Figure 8. (These values represent values used in an actual laboratory setup).

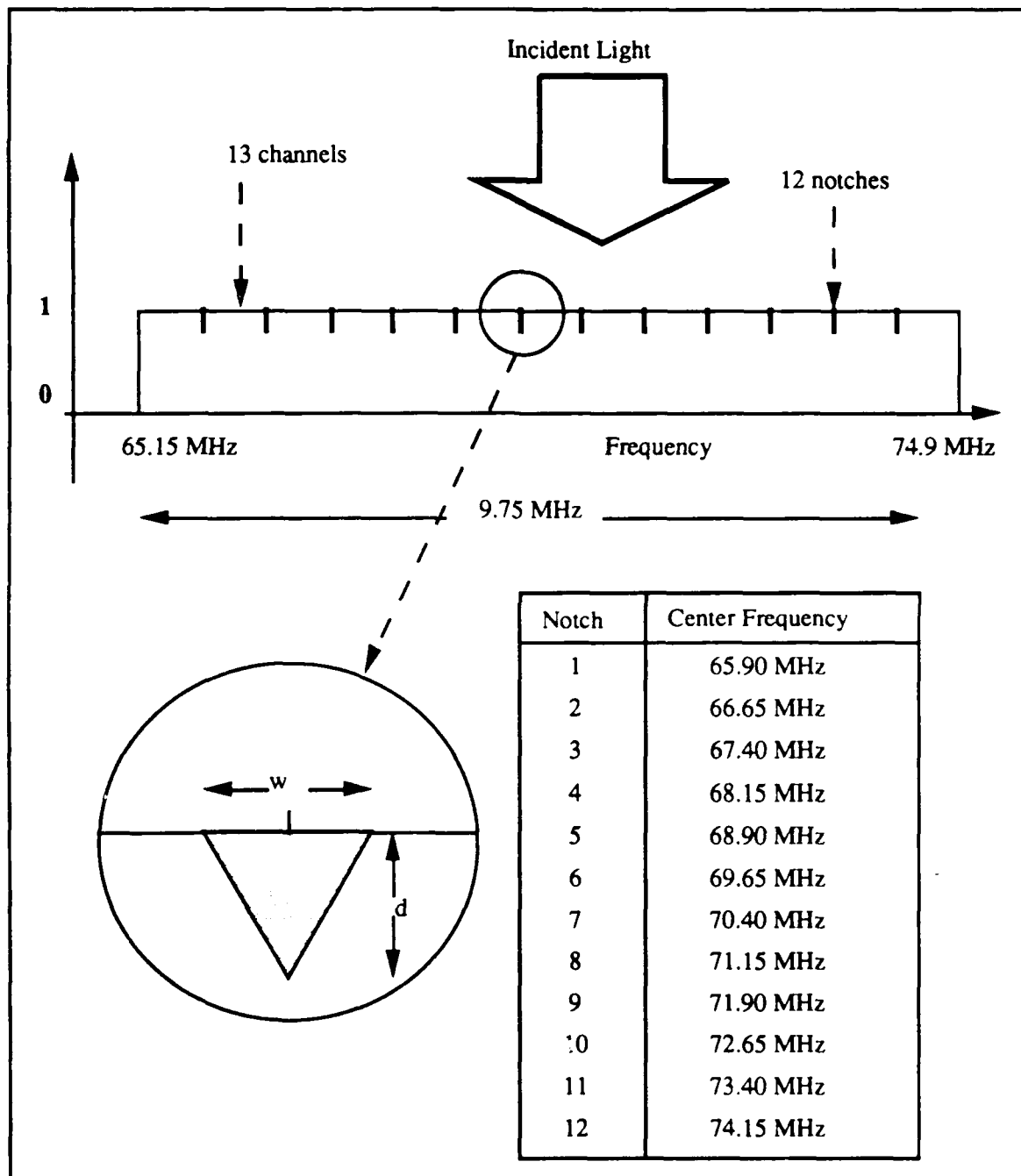


Figure 8 - Excisor-detector array

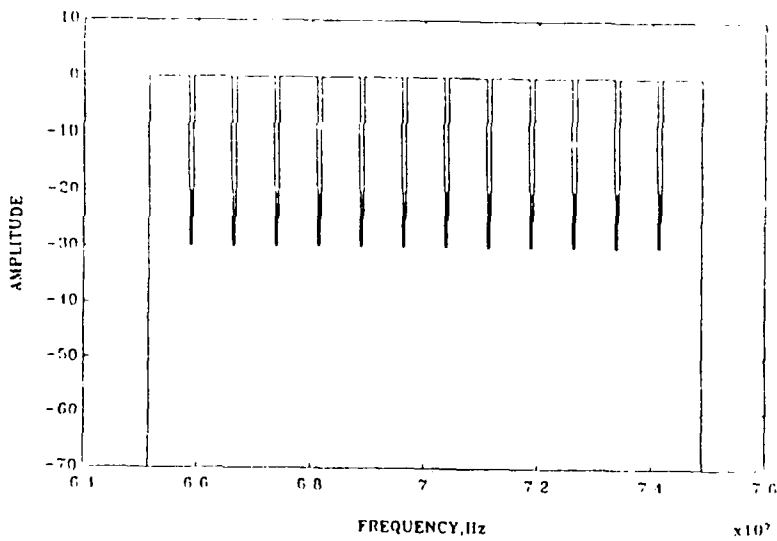


Figure 9 - Filter magnitude response

In the computer program (Appendix B, p. 66) the notch depth is selected to represent the desired attenuation. The separation between points in the frequency domain is 5 KHz. To represent a notch 60 KHz wide, 12 numbers or different elements are needed.

The frequency axis is created considering that the sampling frequency ( $f_s$ ) must be greater than twice the highest frequency present in the signal that is being sampled. That is, the sampling frequency must satisfy the inequality  $f_s > 2f_{\max}$  [Ref. 7]. The highest frequency in our test signal is  $f_{\max} = 70$  MHz, so the sampling frequency must be greater than the Nyquist frequency  $2f_{\max} = 140$  MHz. For the simulation  $f_s = 163.84$  MHz has been chosen.

Using MATLAB386 [Ref. 4] the following expression was used to create the frequency axis:

$$f = (\text{bin\_number} - 1) * fs / N \quad (10)$$

where

$f$  = frequency axis,

$fs$  = sampling frequency,

$N$  = number of points or vector length, and

$\text{bin\_number} = N/2+1$ .

In order to represent the filter signal centered at 70 MHz the values used in the previous expression have been  $N = 32768$ ,  $\text{bin\_number}-1 = 16384$ , and  $fs = 163.84$  MHz.

Two plots are presented on the screen, showing the detector array filter signal and the filter magnitude response.

#### 4 - BLOCK S\_BPSK.m

This block constructs the input test BPSK signal, the interference signal, and the time axis to be used in the program.

The BPSK signal is represented by [Ref. 7]

$$s(t) = A_c \cos[\omega_c t + D_p m(t)] \quad (11)$$

where  $m(t)$  is a bipolar baseband data signal with peak values  $\pm 1$ . Recalling that  $\cos(x)$  and  $\sin(x)$  are even and odd functions of  $x$ , the BPSK signal can be obtain by [Ref. 7]

where the first term is called the pilot carrier term and its level is set by the value of the peak deviation  $\Delta\theta = D_p$ .

For digital angle-modulated signals, the digital modulation index,  $h$ , is defined by [Ref. 7]

$$h = 2 \Delta\theta / \pi \quad (13)$$

where  $2 \Delta\theta$  is the maximum peak-to-peak phase deviation during the time that it takes to send one symbol,  $T_s$ . For binary signaling, the symbol time is equal to the bit time,  $T_s = T_b$ .

The power in the second term (called the data term) needs to be maximized. This is accomplished by letting  $\Delta\theta = D_p = 90^\circ$  [Ref. 7], which corresponds to a digital modulation index of  $h = 1$ . For this case, changing sin by cos, the BPSK signal becomes

$$s(t) = A_c m(t) \cos \omega_c t \quad (14)$$

where

$$\omega_c = 2 \pi f_c, \text{ and}$$

**Ac = Amplitude.**

Equation 14 is the algorithm applied in the test signal generation. The  $m(t)$  signal is a random binary data that represents the modulating waveform originated from a digital information source and is illustrated in Figure 10. The use of random data should be more effective than using any other deterministic method.

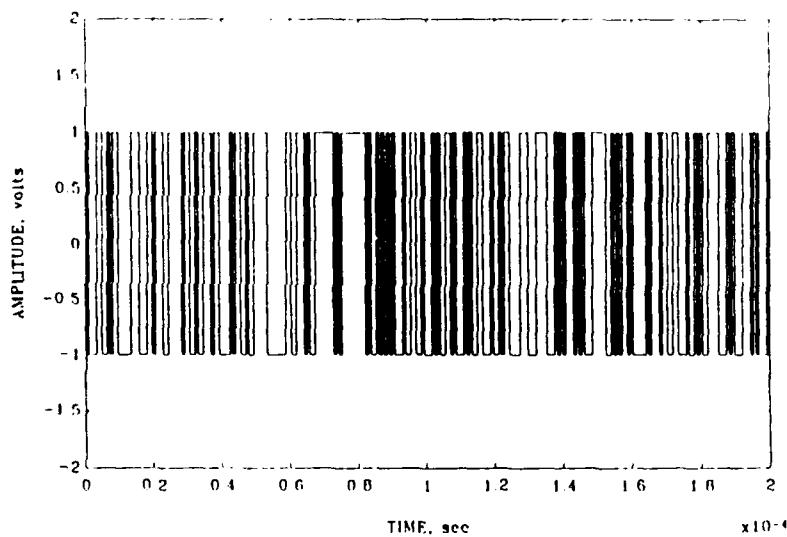


Figure 10 - Binary random data

The random number generator (RNG) employed must fulfill the following requirements [Ref. 8]:

- Uniform: It must pass several statistical test for  $U(0,1)$  uniform distribution.
- Reproducible: To be useful, the RNG should reproduce the same string of numbers given the same seed every time; this is of particular importance for testing purpose.
- Minimum Memory: It should be efficient to use and fast.
- Non-repeating: A number sequence must not repeat itself during a simulation run.
- Statistical Independent: This property is very difficult to achieve because of the recursive properties of the generator.

The mathematical algorithm was based on the linear congruential method of the form [Ref. 8]:

$$z_i = (a \cdot z_{i-1} + c) \text{ MOD } m \quad (15)$$

where

a = multiplier,  
c = increment,  
m = modulus, and  
 $z_0$  = seed.

It can be shown that the pseudorandom number generator can be constructed using the following expression [Ref. 8]

$$z_i = (16807 \cdot z_{i-1}) \text{ MOD } 2^{31}-1 \quad (16)$$

For the random case the test signal generated by Eq. 14 will produce a continuous spectrum as will be presented later.

The interference signal is also generated in the present block based on a sinusoidal signal with an amplitude three times the original BPSK signal (in the time domain) and a carrier frequency selectable from the input data. As a result of adding those two signals, the test BPSK signal plus interference is produced.

The generation of the time axis is other function of this block. A total time of 0.2 milliseconds with intervals of 6.1 nanoseconds has been selected.

Plots presenting the random binary data, BPSK test signal, and BPSK test signal plus interference are presented on the screen as

shown in Figures 11 and 12. A carrier frequency of 70 MHz and an amplitude of 1 volt was used for the BPSK signal and a central frequency of 67.4 MHz and 3 volts amplitude for the interference signal.

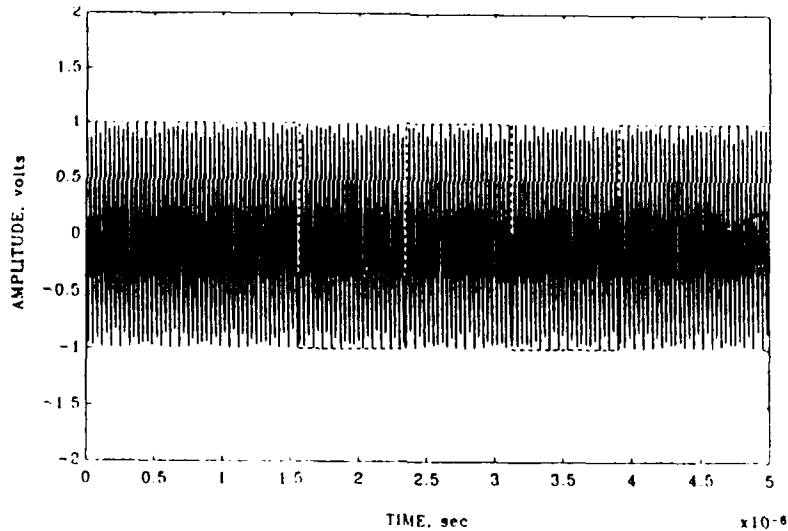


Figure 11 - BPSK signal and modulated waveform

## 5 - BLOCK FFT\_B.m

The FFT\_b.m block uses the input signal constructed in the previous block and calculates the fast Fourier transform. The first step in applying the discrete Fourier transform is to choose the number of samples N and the sampling interval T, and, secondly, to interpret the results correctly. The discrete transform approximates the continuous transform rather poorly for the higher frequencies [Ref. 7]. To reduce this error it is necessary to decrease the sample interval T and/or to increase N.

In our case the relationship used was

$$T = \text{Period} / N \quad (17)$$

where

$N = 32768$  ( $N = 2^\varphi$  where  $\varphi$  is an integer value), and

Period = 0.2 millisec.

So  $T = 6.1$  nanosec.

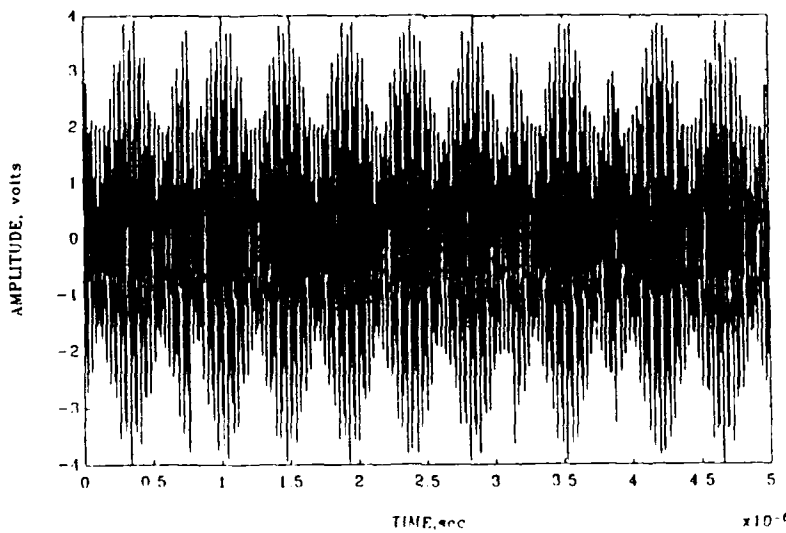


Figure 12 - BPSK signal plus interference

From MATLAB386 [Ref. 4] the  $\text{FFT}(x)$  is the discrete Fourier transform (DFT) of vector  $x$ , computed with a radix-2 fast Fourier transform algorithm. If the length of  $x$  is not an exact power of two then it is padded with trailing zeros. This is not our case because we have selected  $N = 32768 = 2^{15}$ .

The function that implements the transform is given by

$$X(k+1) = \sum_{n=0}^{N-1} x(n+1) W_N^{kn} \quad (18)$$

where  $W_N = e^{-j(2\pi/N)}$  and  $N = \text{length}(X)$ . Note that the series (18) is written in an unorthodox way, with the subscript from  $k+1$  instead of the usual  $k$  because subscripts on Matlab vectors run from 1 to  $N$  instead of from 0 to  $N-1$  [Ref. 4].

In order to plot the FFT results, the frequency axis generated in the Filter.m block is used. Actually the power spectral density (PSD) is calculated and plotted as shown in Figures 13.

Also, for comparison purposes, the theoretical power spectral density of a BPSK signal with the same characteristics as the test signal was calculated and plotted using the following algorithm:

$$P(f) = \frac{A_c^2}{4R} \left\{ \frac{\sin(\pi(f - f_c)T_b)}{\pi(f - f_c)T_b} \right\}^2 \quad (19)$$

where

$T_b$  = bit time =  $1/R$ , and

$R$  = bit rate.

The resulting BPSK spectrum is shown in Figure 14. The null-to-null bandwidth is  $2R$ . The figure shows plots of the calculated and the theoretical PSD of the test signal. As we can see, the calculated spectrum (solid line) appears to be noisy but follows the theoretical spectrum plotted using equation 19 (dotted line). Therefore the algorithm used is a good representative of a BPSK signal.

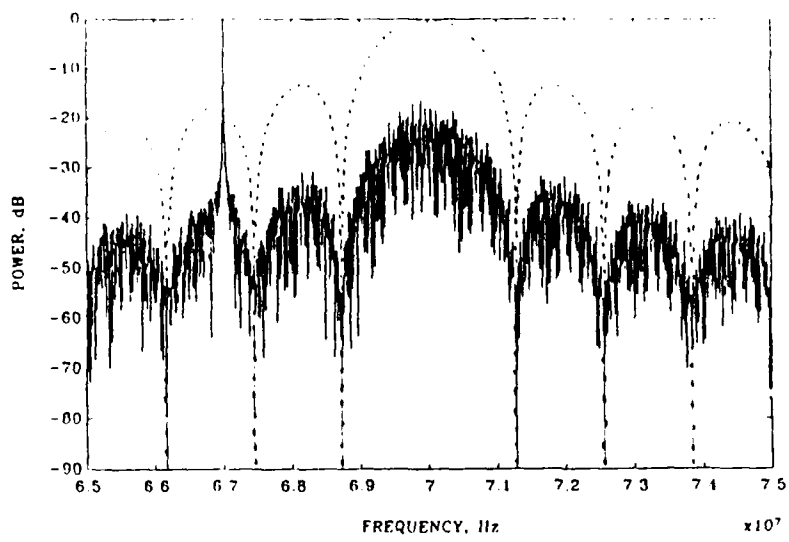


Figure 13 - PSD of a test BPSK signal plus interference

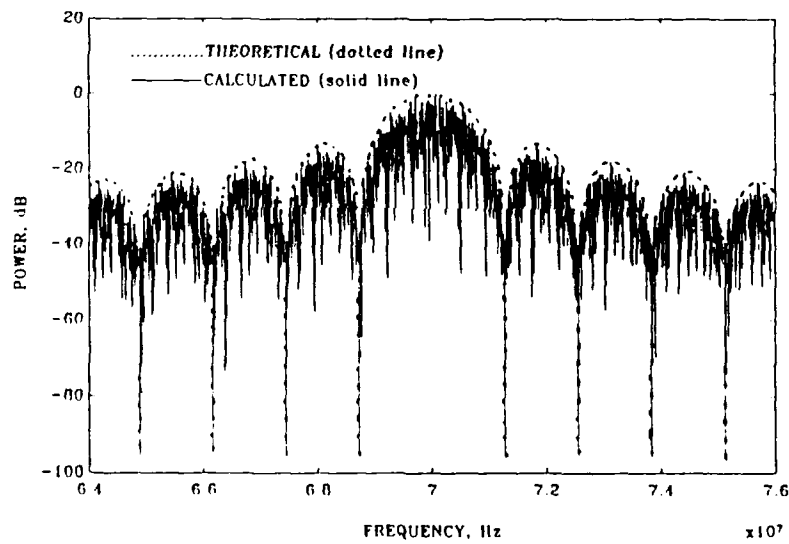


Figure 14 - Theoretical and calculated PSD of a BPSK signal

## 6 - BLOCK S\_FIL.m

The purpose of this block is to take the FFT of the input signal and multiply it with the detector array filter. As stated

before, the photodiode array with the small space between each of the photodiodes can produce the filter. Placing a notch where the interference is present produces a narrowband frequency rejection via a notch filter. Also the harmful effect of notches on the other frequency components of the original signal must be considered.

A plot of the filter transfer function and the test signal spectrum will be presented in order to visualize the effect of the filter on the signal.

Finally a comparison between the filtered signal spectrum and the original signal spectrum is showed to evaluate a priori the filtering effect.

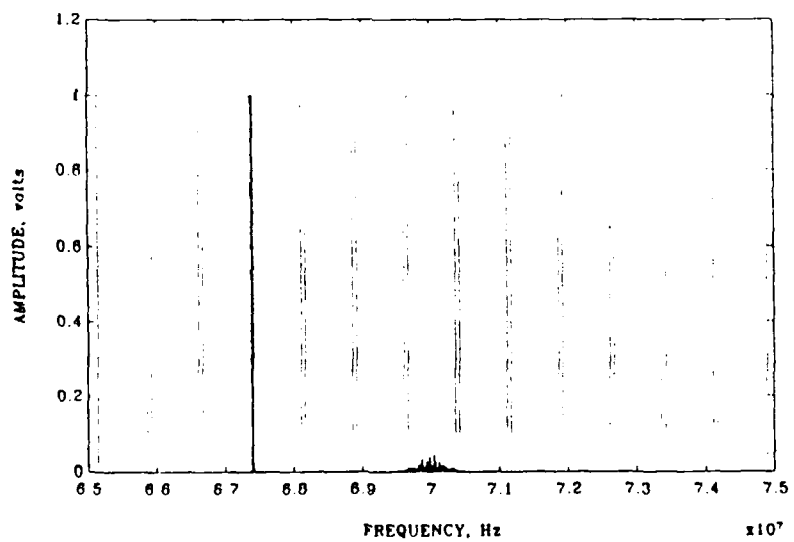
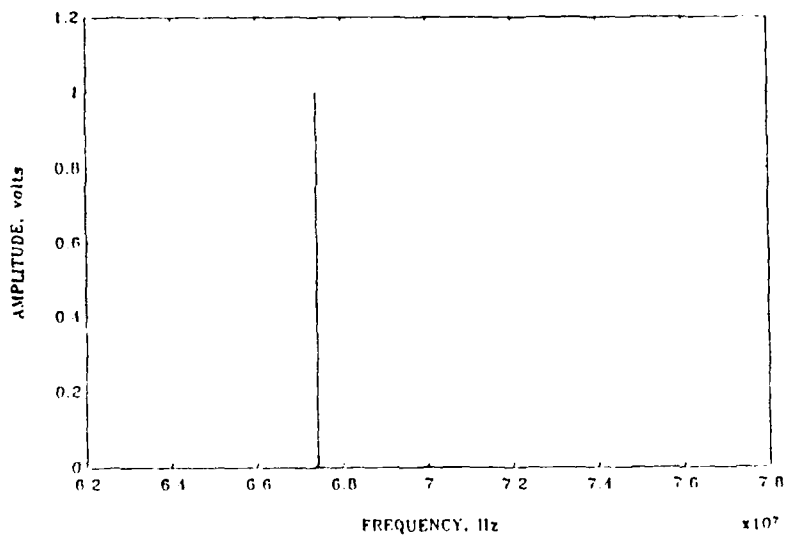


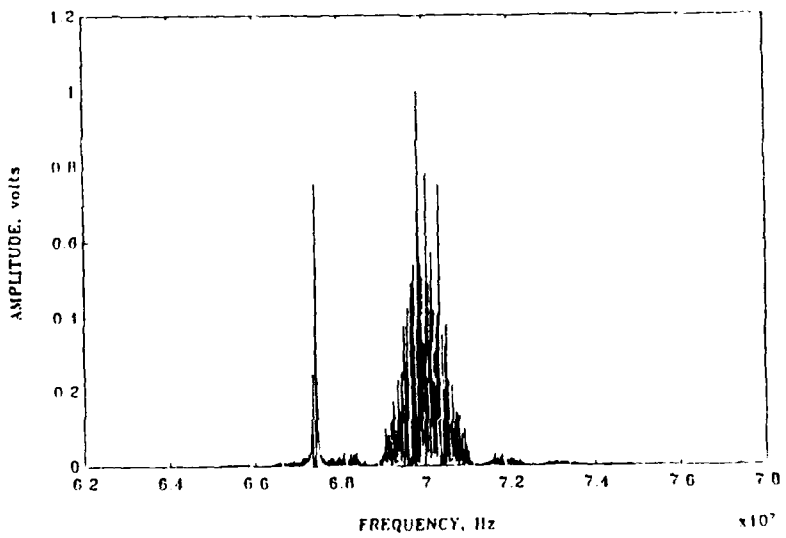
Figure 15 - Filter transfer function and test signal spectrum

An example of these plots are illustrated in Figures 15 and 16. In Figure 15 the interference dominates the spectrum and the BPSK

signal appears relatively small. Also the magnitude of the filter response of the excisor-detector array is shown. The overlap of the interference with the third notch is clearly shown. After the filtering process takes place (Figure 16b), the BPSK signal increases with respect to the interference signal, showing the effectiveness of the filtering process.



a - Original signal spectrum



b - Filtered signal spectrum.

Figure 16 - Filtered and original signal spectrum comparison

## 7 - BLOCK IFFT\_B.m

Here the output signal is determined by an inverse transform of the filtered signal calculated in the previous block. In order to perform the inverse fast Fourier transform (IFFT) the following algorithm was used [Ref. 4]:

$$x(n+1) = \frac{1}{N} \sum_{k=0}^{N-1} X(k+1) W_N^{-kn} \quad (20)$$

The recovered signal is presented and compared with the original test BPSK signal without interference as shown in Figure 17.

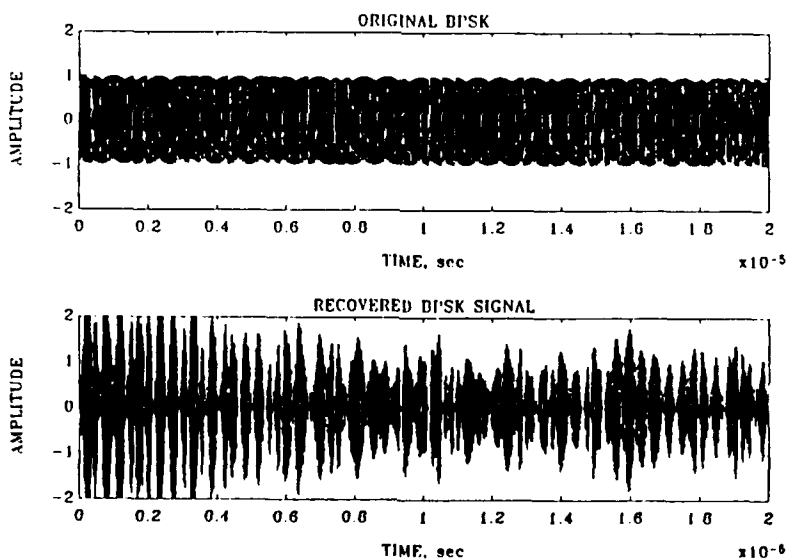


Figure 17 - Original and recovered BPSK signal

We can see that the recovered signal experiences a distortion due to the notches and the windowing effect of the excisor-detector array, in addition to the interference signal.

## 8 - BLOCK COD\_B.m

The optimum detection of a BPSK signal consists of coherent detection as showed in Figure 18. The gated integrator that is turned on at the beginning of each bit period ( $T_b$ ) and integrates to the end of the bit. Then the integrator output is sampled and mapped into digital values (a binary 1 if the sample value is a positive voltage and a binary 0 if the sample value is negative). The integrator is then reset to a zero initial condition and this procedure is repeated for detection of the next bit. This optimum detector is called an integrate and dump detector [Ref. 7] presented in Figure 19.

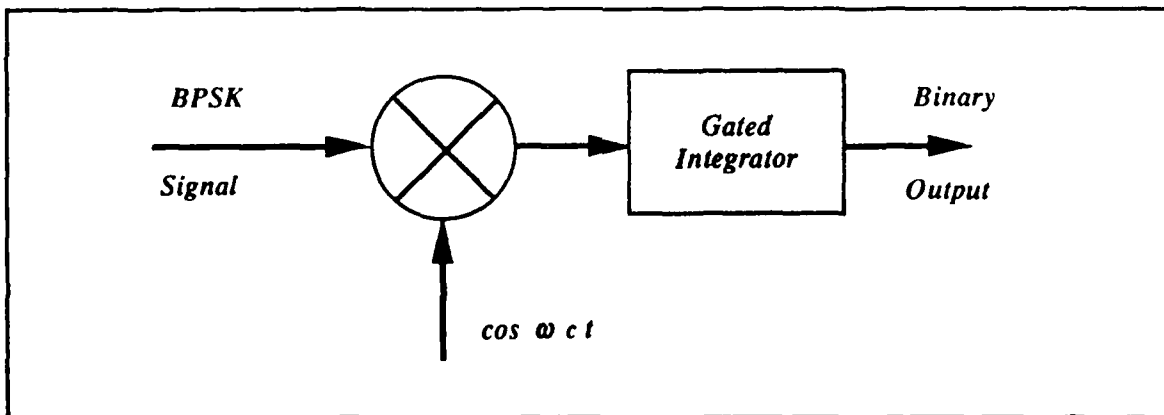


Figure 18 - Coherent detection

The operation described is simulated with a FOR loop that computes the cumulative sum during the bit time and is dumped to zero at the end. To map the integrator output (Figure 20) into

digitals values, another loop with logic statements is performed, reading the middle point of each bit time. These operations generate a string of binary data that will be compared to the original random binary information as shown in Figure 21.

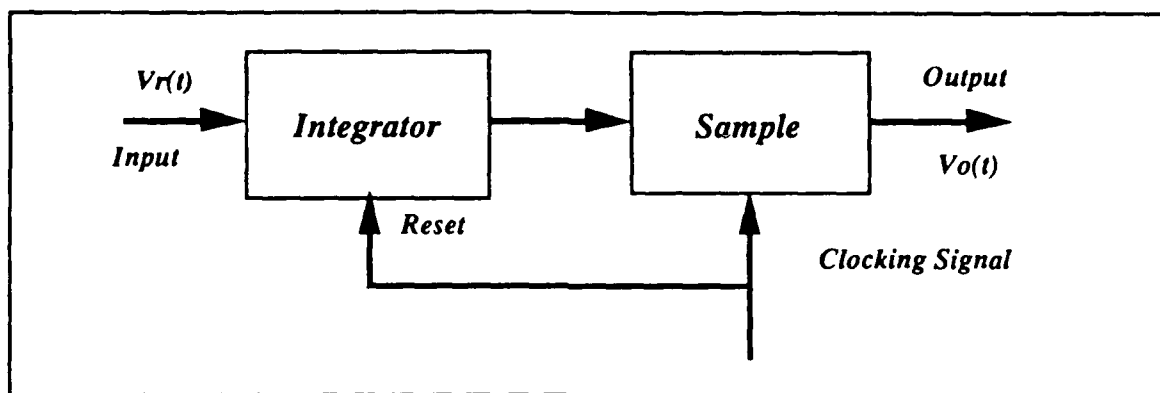


Figure 19 - Integrate and dump detector

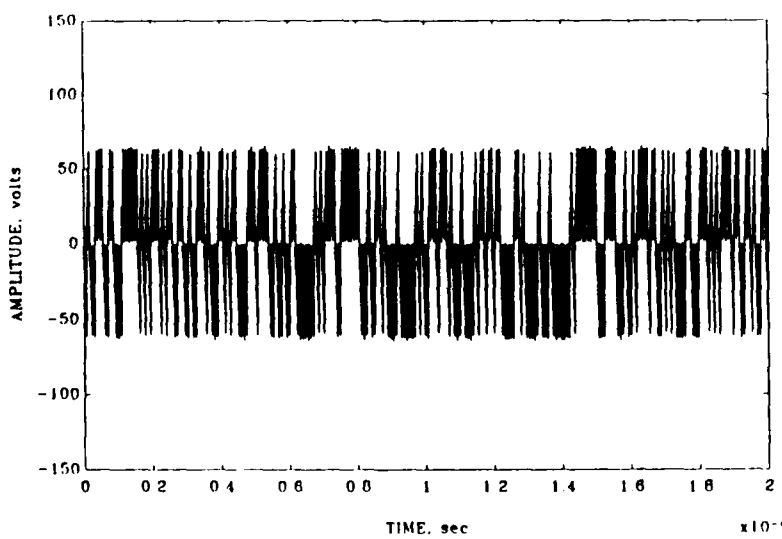


Figure 20 - Integrator output ( $T_b = 0.78 \mu\text{sec}$ )

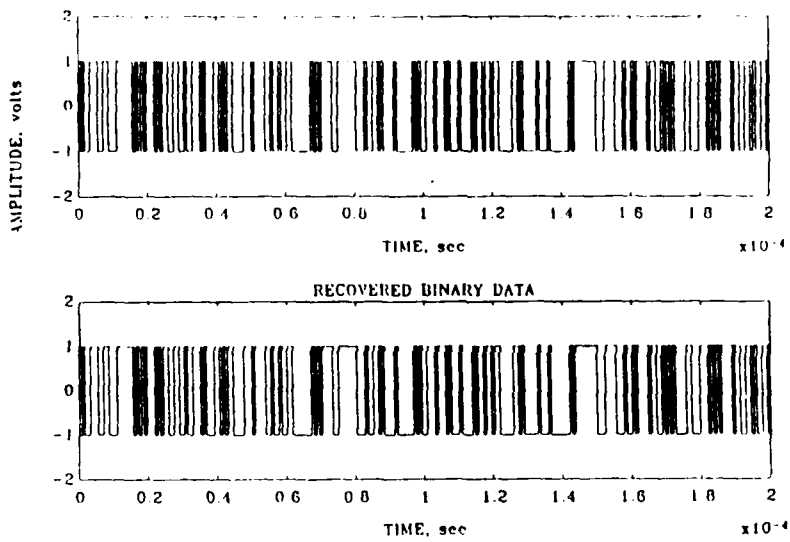


Figure 21 - Original and recovered binary data.

In order to detect if an error is present, the original random binary data and the recovered binary data are compared. This information is presented on the screen showing a 1 if no error is detected otherwise a -1 represents an error (Figure 22).

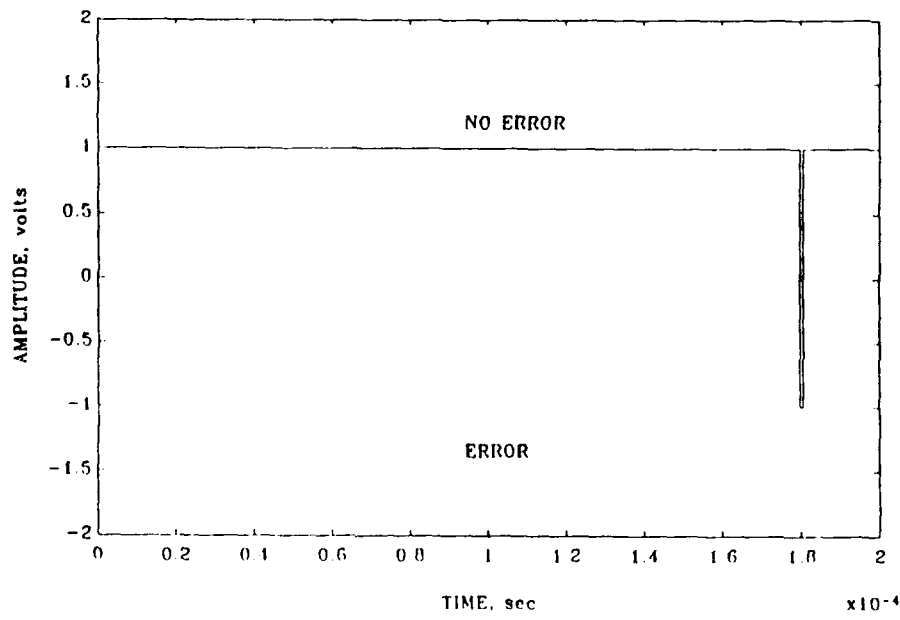


Figure 22 - Error detection

If in the input data the number of intervals (I) selected is greater than 1, the program regenerates a test BPSK signal with the interference frequency shifted an amount equal to the frequency interval (delta) introduced at the INP\_B.m block. This action simulates the movement of the excisor-detector array in order to evaluate the effect of this translation on the output signal.

## V. PROGRAM EVALUATION

An evaluation of the computer program presented in Chapter IV and Appendix B was performed under different conditions as shown in Table II. The main idea was to be sure that the output for each test agreed with what we expected or with previous experimental results.

TABLE II - TEST CONDITIONS

Test Signal \ Excisor-detector	YES with notches	NO without notches
BPSK signal without interference	<i>Degradation of the original signal due to notches</i>	<i>Degradation of the signal passing through the window</i>
BPSK signal with interference	<i>Filtering capability over the interference</i>	<i>Degradation of the signal. Errors on the Data recovered</i>

### A- TEST N° 1

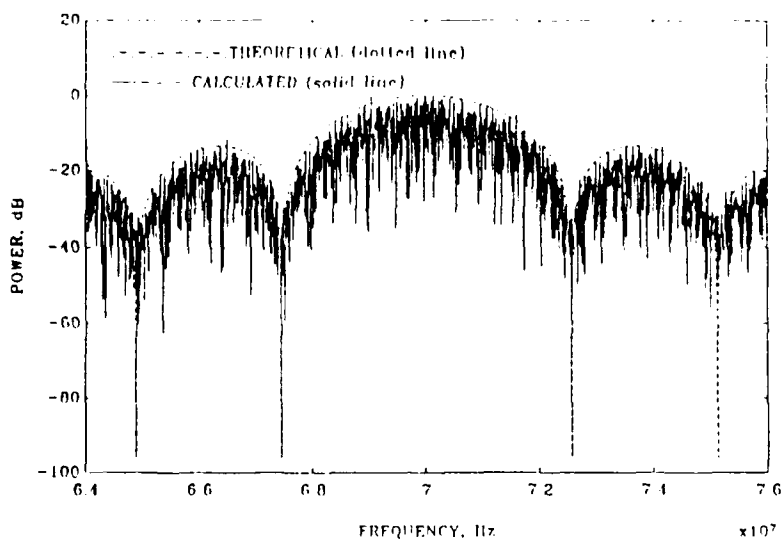
For the purpose of the test, a BPSK signal without interference was considered. An excisor-detector array without notches (ideal, as a window 9.75 MHz wide using an attenuation factor of 1 (0 dB)) was

used to represent the detector array centered at 70 MHz. The BPSK signal generated as a test signal had the following parameters that remained constant during all other tests.

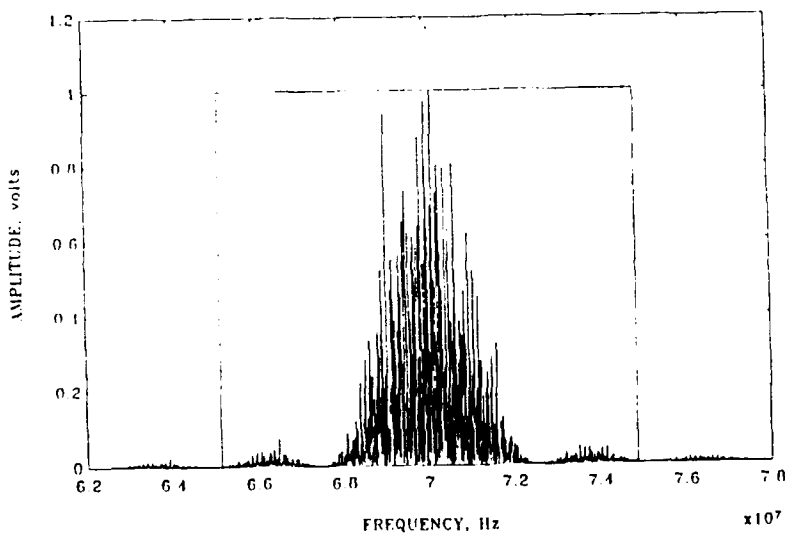
TABLE III - TEST SIGNAL PARAMETERS

Parameter	Description	Value
A	Amplitude BPSK signal	1 volt
Ai	Amplitude interference	3 volts
Tb	Bit Time	0.39 $\mu$ sec
fc	Carrier Freq. BPSK	70.0 MHz
fi	Center Freq. Interference	67.4 MHz
seed	PRNG seed number	236578

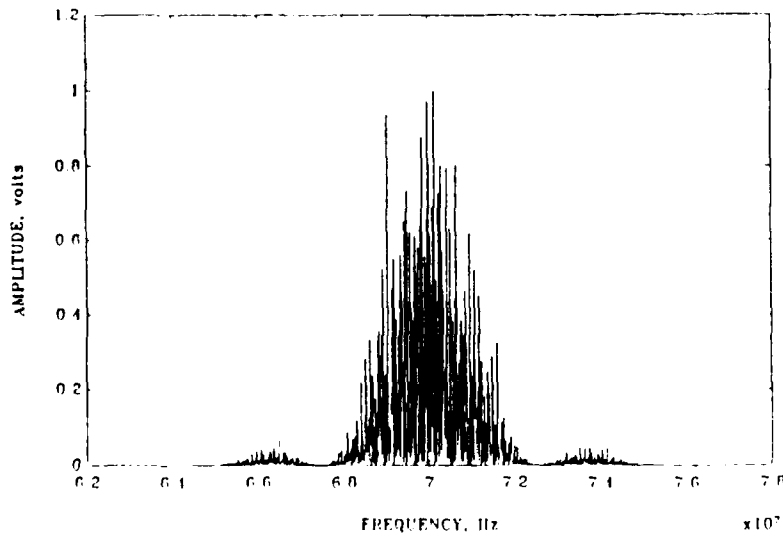
In the first test the central frequency of the interference was selected as  $f_i=0$  in order to simulate a no-interference. The value of the bit time ( $T_b$ ) equal to 0.39  $\mu$ sec was employed to put the minimal amount of the original signal on the window (main lobe and the first side lobes). The results of this simulation are summarized below (Figure 23) and match what was expected.



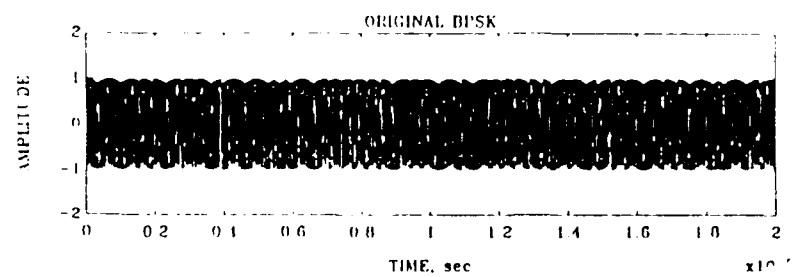
a- PSD of the Test signal. The theoretical PSD is shown in dotted line and the calculated in solid line.



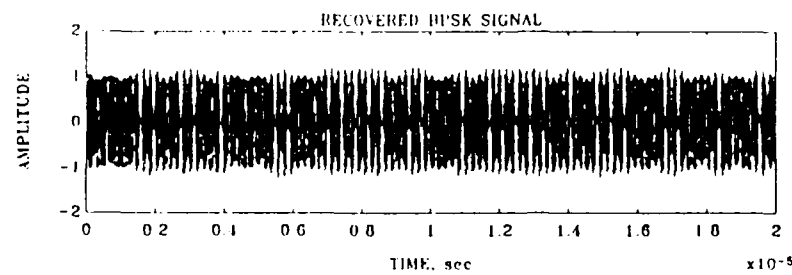
b- Filter (excisor-detector array) signal and the spectrum of the test signal.



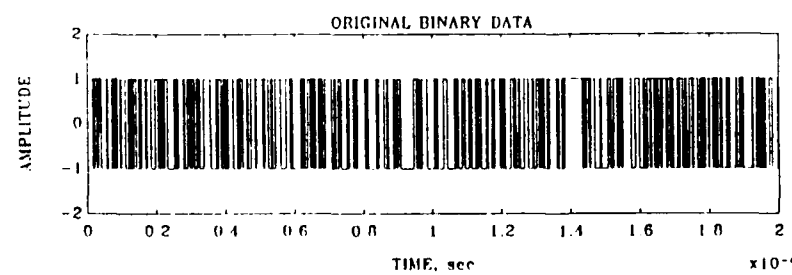
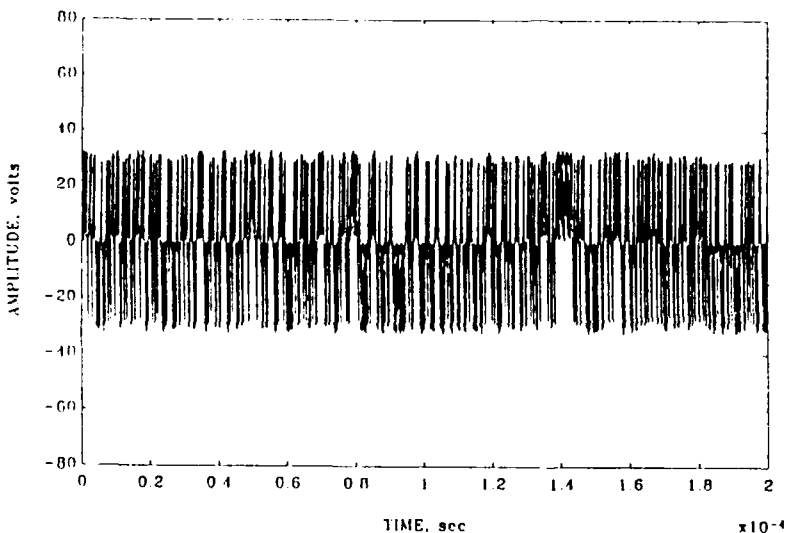
c- Spectrum of the test BPSK signal after filtering (frequency domain).



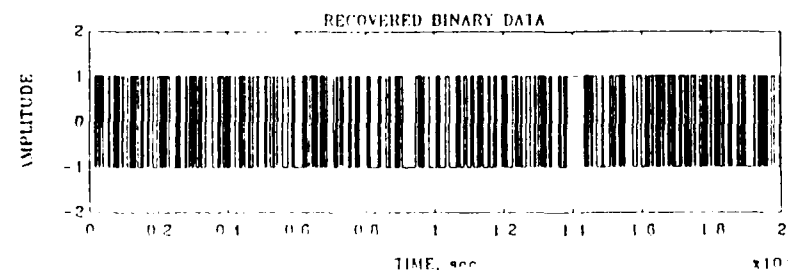
d- Recovering the BPSK signal and comparing it with the original test BPSK signal.



e- Integrator output during the detection process.



f- Plot of the original Random Binary Data  $m(t)$  and the recovered data after the process.



g- Checking for  
bit error.

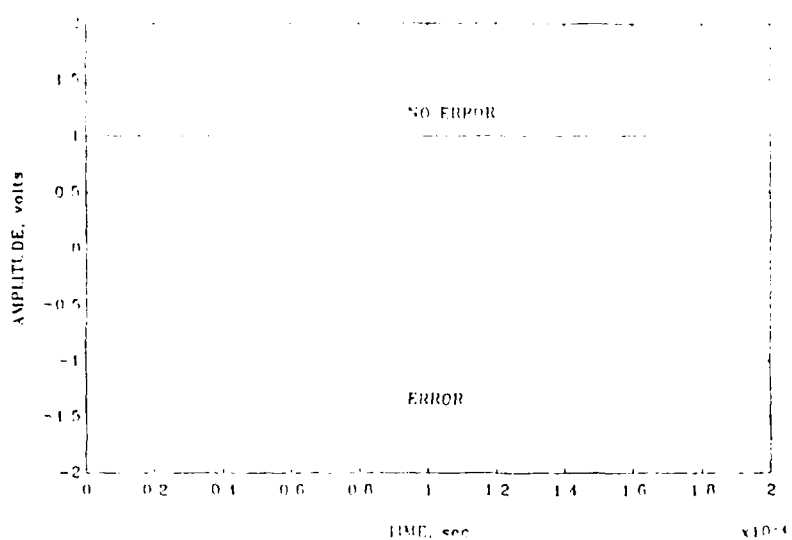
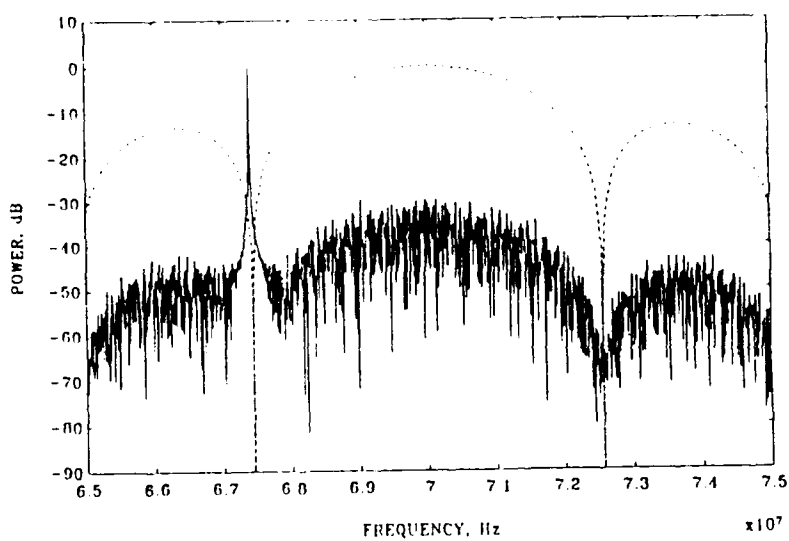


Figure 23 - Output Test N° 1

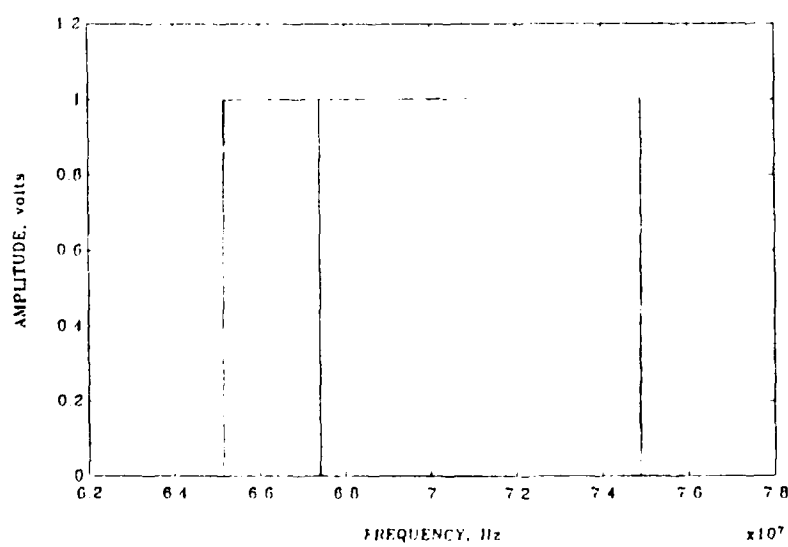
As was expected the degradation of the test BPSK signal due to the window 9.75 MHz wide was very small and the data information was recovered without any error.

#### B- TEST N° 2

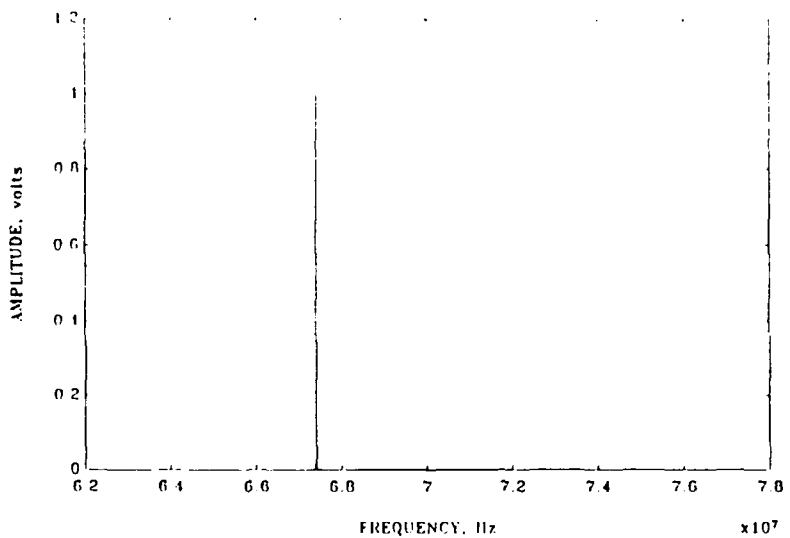
The second test used the same test BPSK signal as before with the addition of an interference. The excisor-detector was still a window 9.75 MHz wide with an attenuation factor of 1 (0 dB). Figure 24 shows the results of Test N° 2.



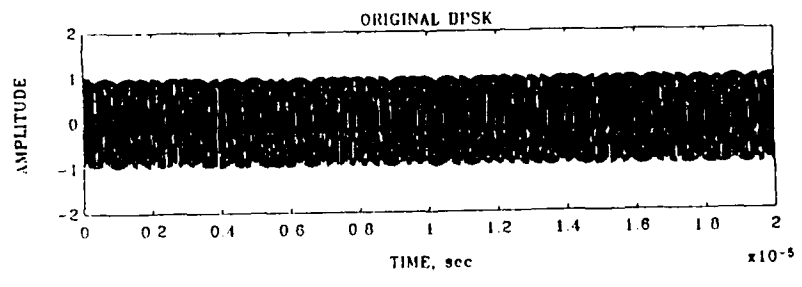
a- PSD of the test BPSK signal plus interference is presented in solid line. Theoretical plot is shown in dotted line as a reference. The interference is 30 db above the test signal.



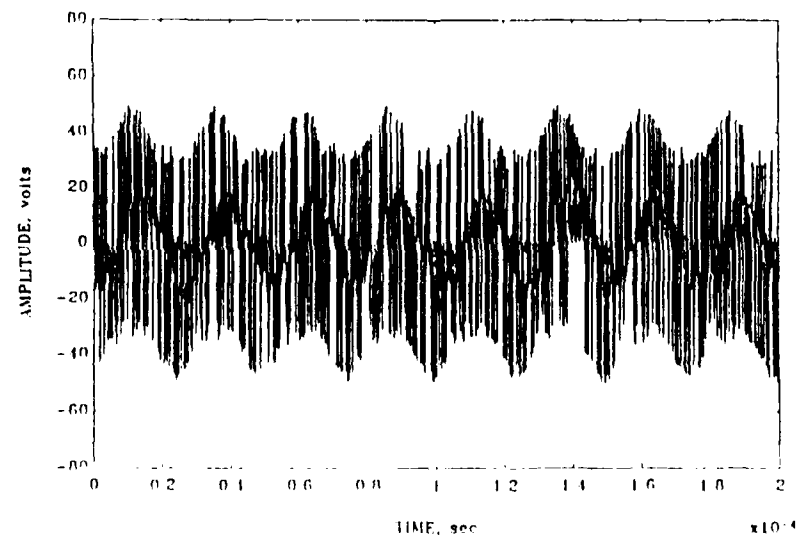
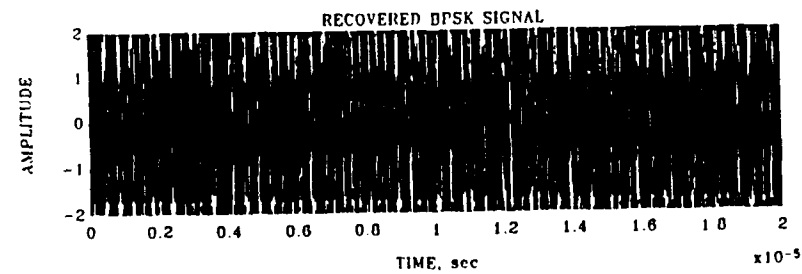
b- Filter signal and spectrum of the test BPSK signal plus interference is presented. Note that the interference signal dominates the spectrum when a linear scale is used.



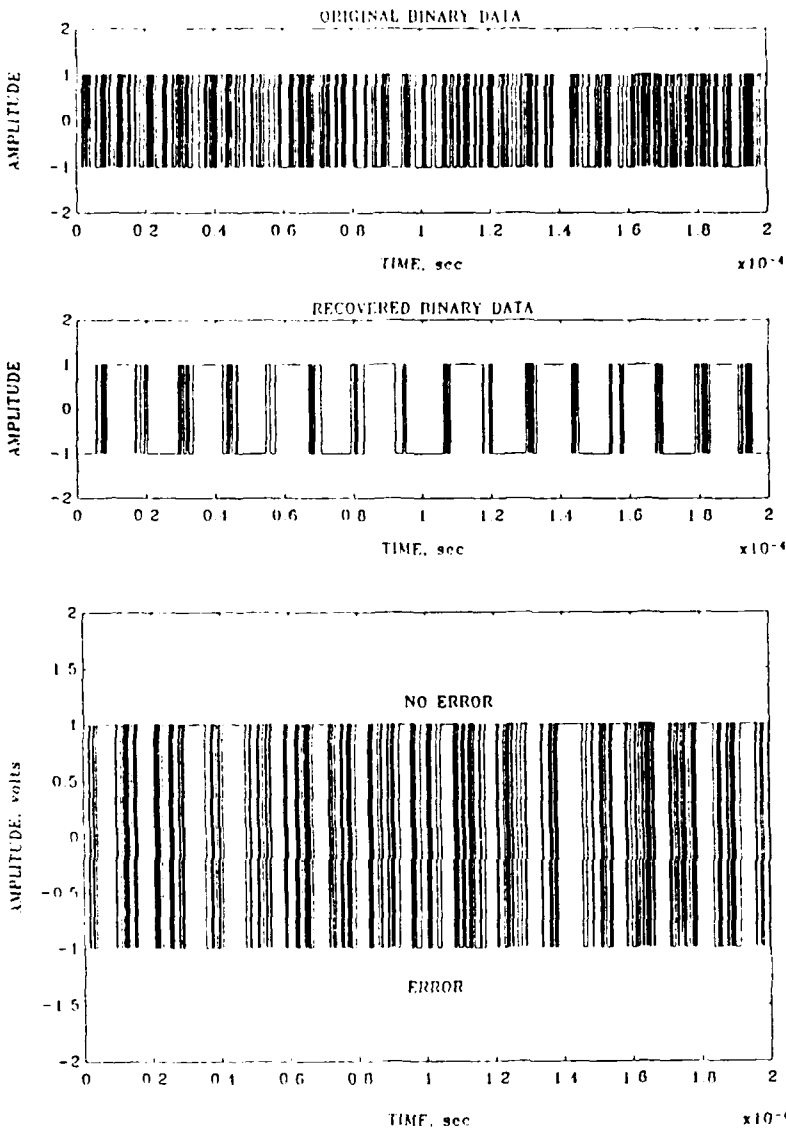
c- Output after  
passing the test  
signal through  
the window.



d- Recovering the  
BPSK signal and a  
comparison with  
the original test  
signal without  
interference is  
shown.



e- Output of  
integrating  
detector.



f- Comparison of the original random binary data  $m(t)$  and the recovered data.

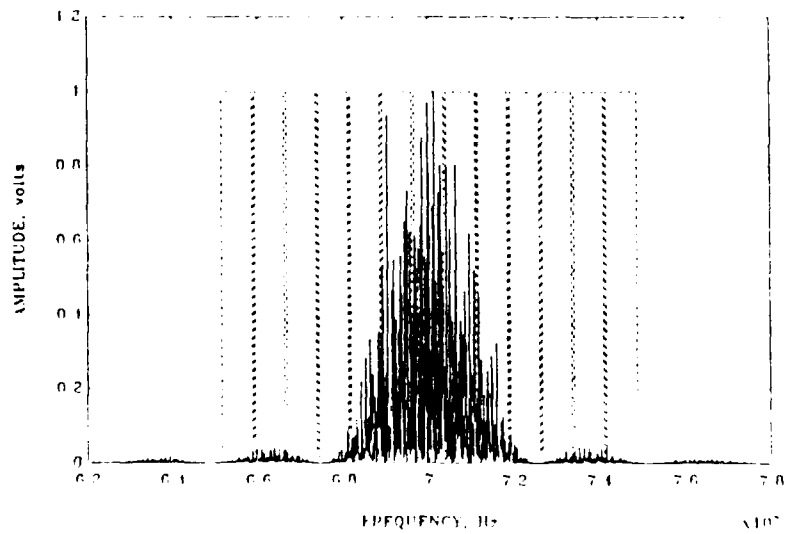
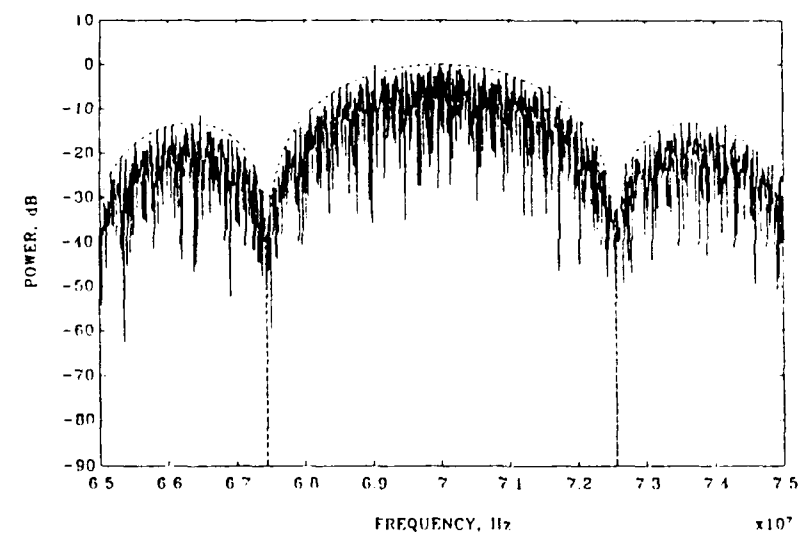
g- Error detection output.

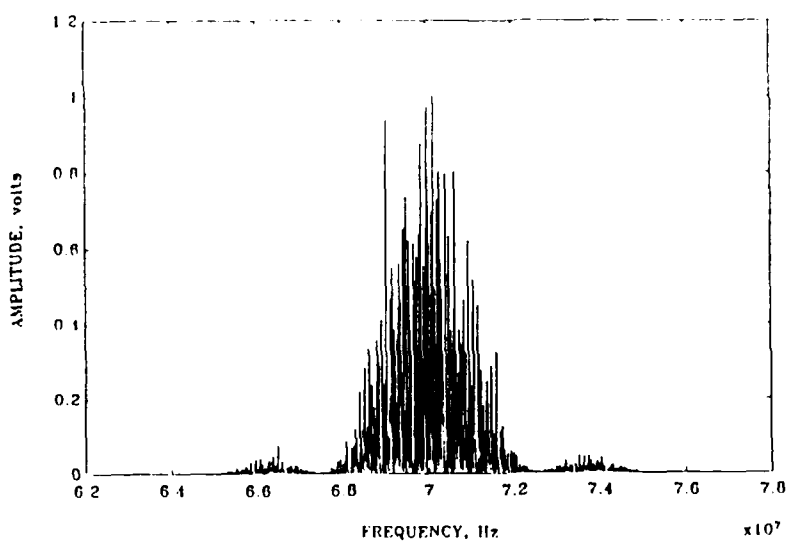
Figure 24 - Output Test N° 2

As seen in Figures 24f and 24g, the interference signal produces a significant distortion on the recovered BPSK signal as well as on the random binary data. Hence a filter is desired to reduce the harmful interference.

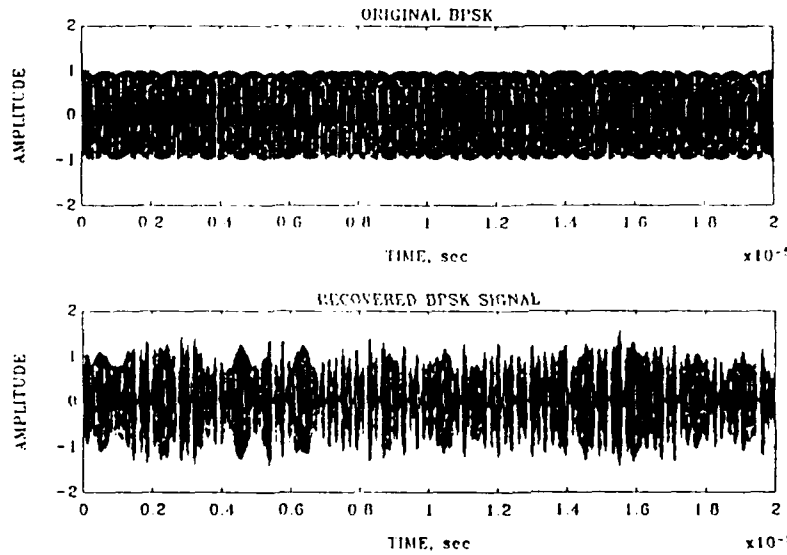
### C- TEST N° 3

From the previous results an effective filtering process is needed. The actual excisor-detector array will have notches in the frequency domain. We want to examine the effects of these notches on the BPSK signal alone. The present test was performed with a test BPSK signal without interference passing through an excisor-detector with notches 60 KHz wide and with a depth of 20 dB (see Figure 25b).

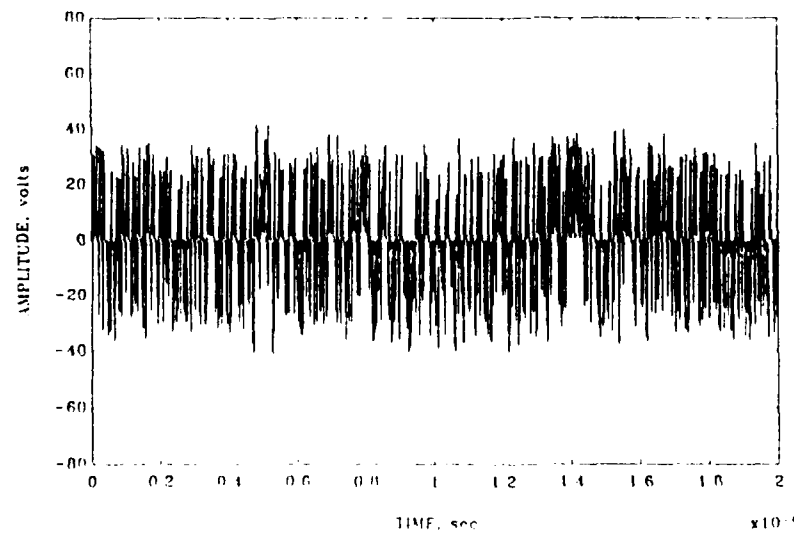




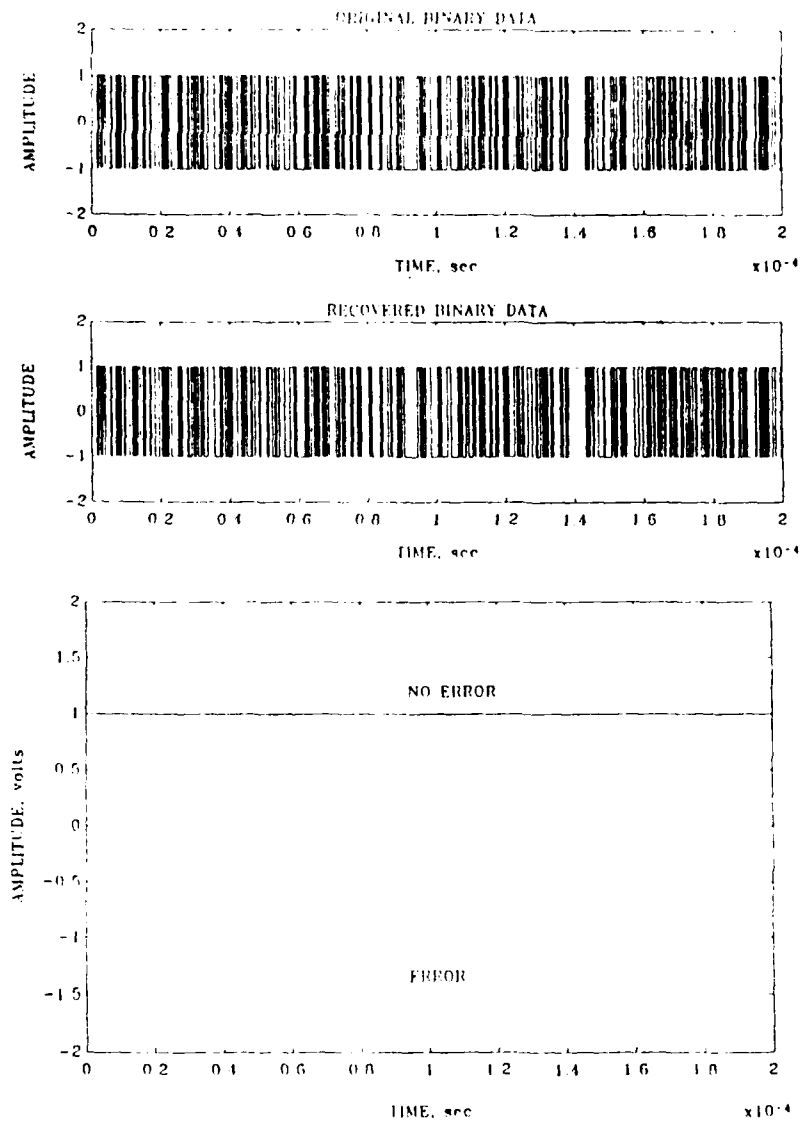
c- After passing through the excisor-detector filter signal the spectrum of the filtered signal is presented.



d- Comparison between the original and recovered BPSK test signal.



e- Integrator output during the detection process.



f- Recovered  
binary data and  
original  $m(t)$   
signal  
comparison.

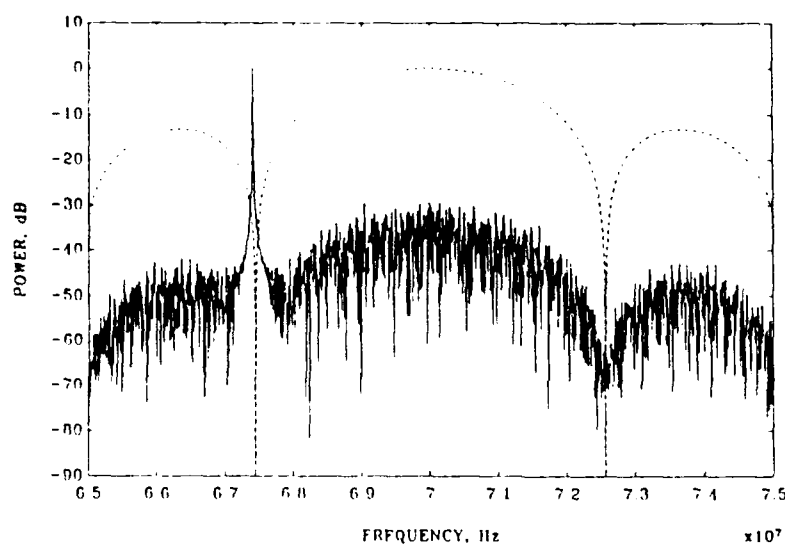
g- Bit error  
detection.

Figure 25 - Output Test N° 3

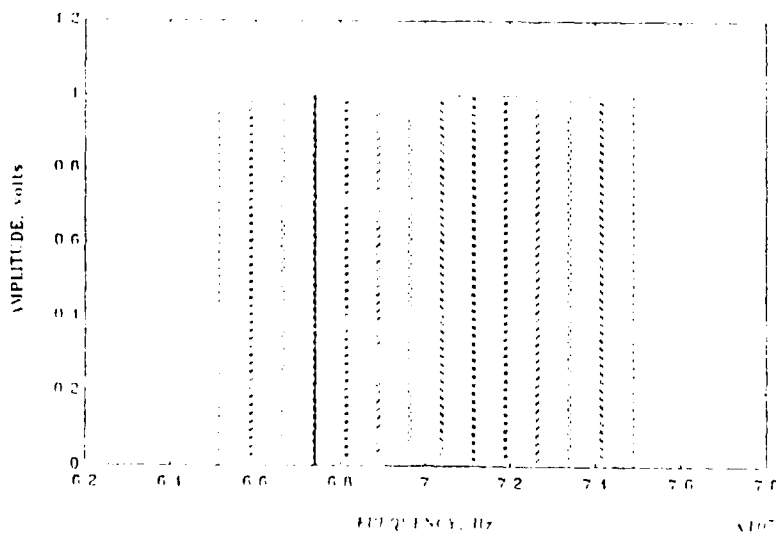
No significant distortion was observed between the results of this filtered signal and the unfiltered BPSK signal (Test N° 1). It is reasonable to state that the effect of these notches (60 KHz wide and 20 dB depth) is negligible on the broadband signal.

## D- TEST N° 4

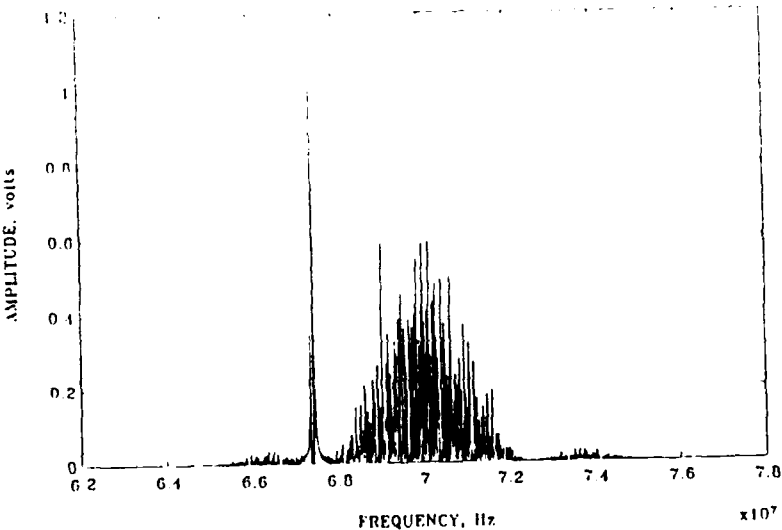
Finally we consider a common situation. The test BPSK signal was considered with an interference present and the excisor-detector array had notches between detectors that will produce the filtering effect. A notch was aligned on the interference frequency (see Figure 26b).



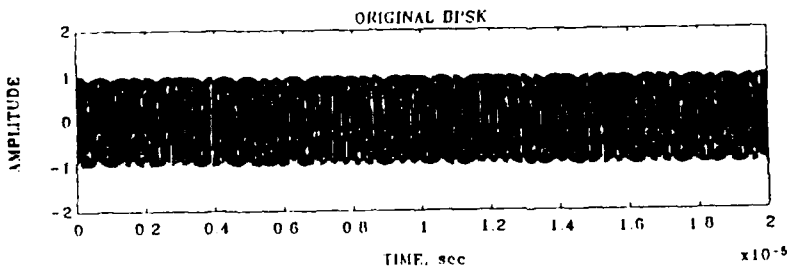
a- PSD of a test BPSK signal with an interference at 67.4 MHz (solid line) and the theoretical PSD of a BPSK signal as a reference.



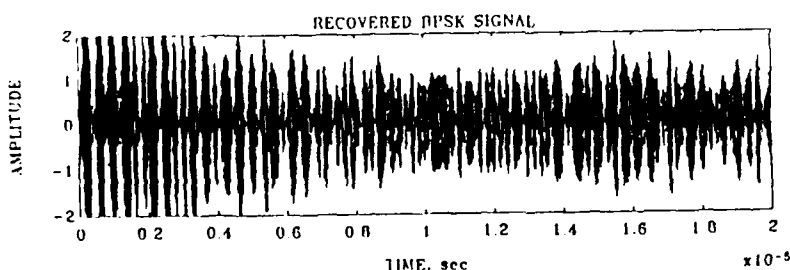
b- Excisor-detector array signal (frequency domain) and spectrum of the test BPSK signal plus interference. Note the interference at the center of the third notch.



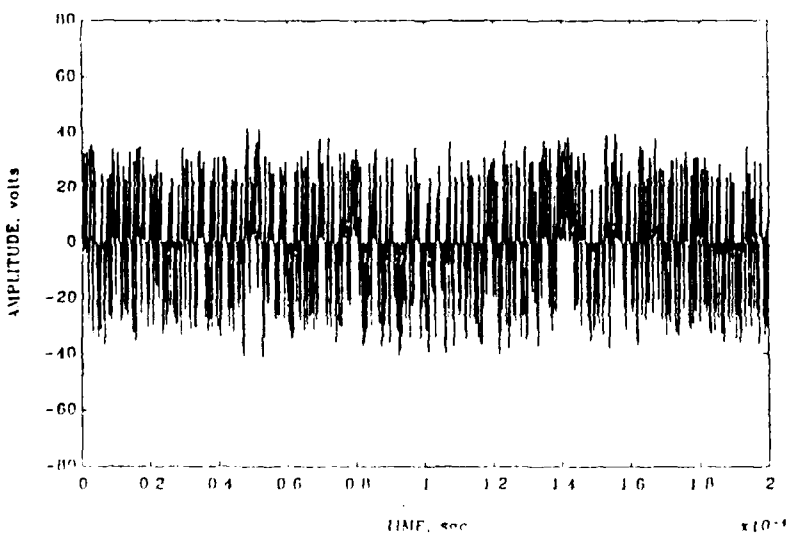
c- Spectrum of the filtered signal. The interference is attenuated and the signal spectrum increases, relative to the interference.

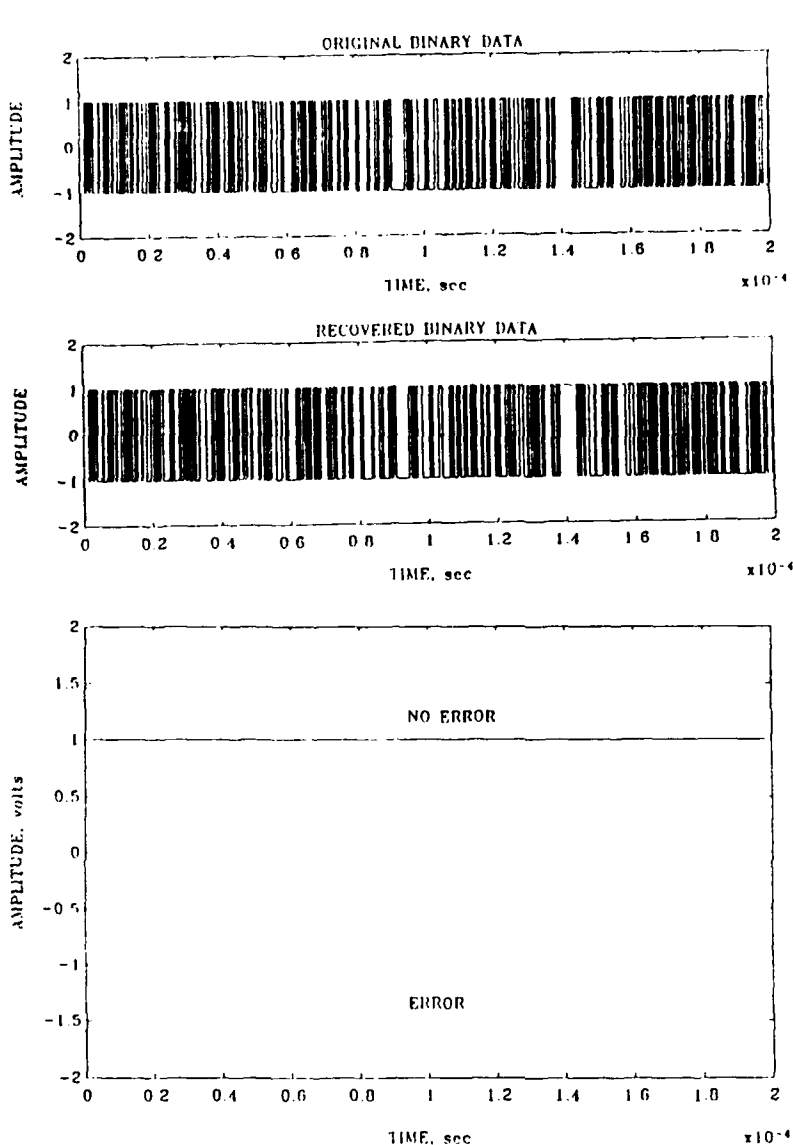


d- The recovered filtered BPSK and the original signal without interference.



e- The integrator detector output.





f- The original data and the recovered data.

g- Error detection between recovered data and test data is performed.

Figure 26 - Output Test № 4

During this test the effect of the narrowband notches was evaluated showing that this filtering technique was effective against the narrowband interference signal considered.

## E- OTHER TESTS

### 1 - NO-FILTER TEST

An early test was performed to check the computer program. The test signal was the BPSK signal without interference. No filtering process was included. We only generated and recovered the BPSK signal (Appendix B, p. 66). The signal was recovered without any distortion (Figs 27, 28 and 29).

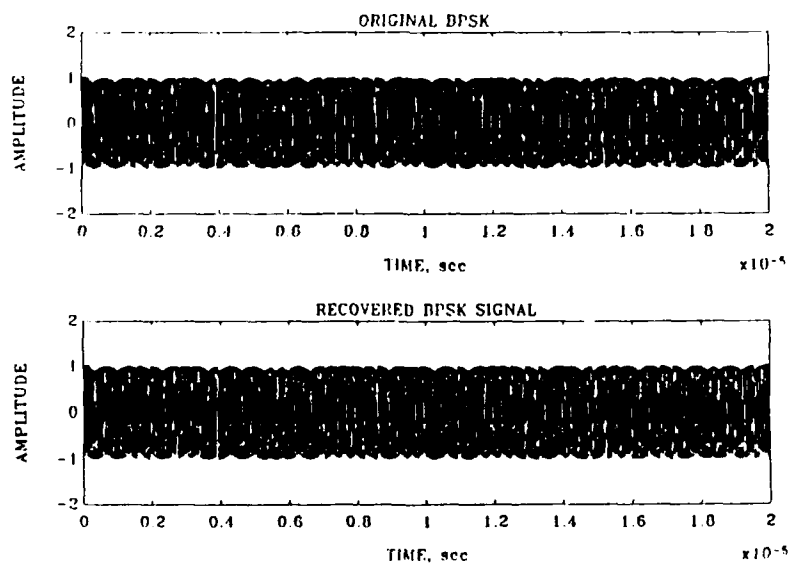


Figure 27 - Original and recovered BPSK signal

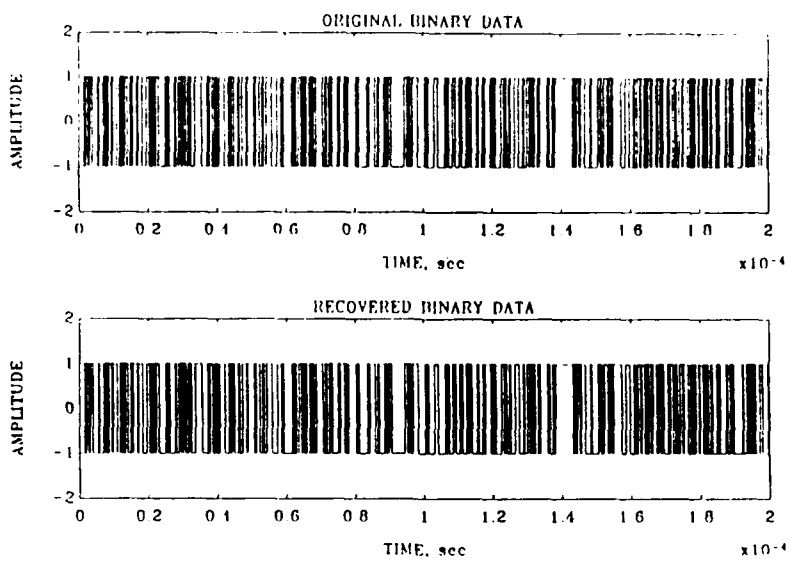


Figure 28 - Original and recovered binary data

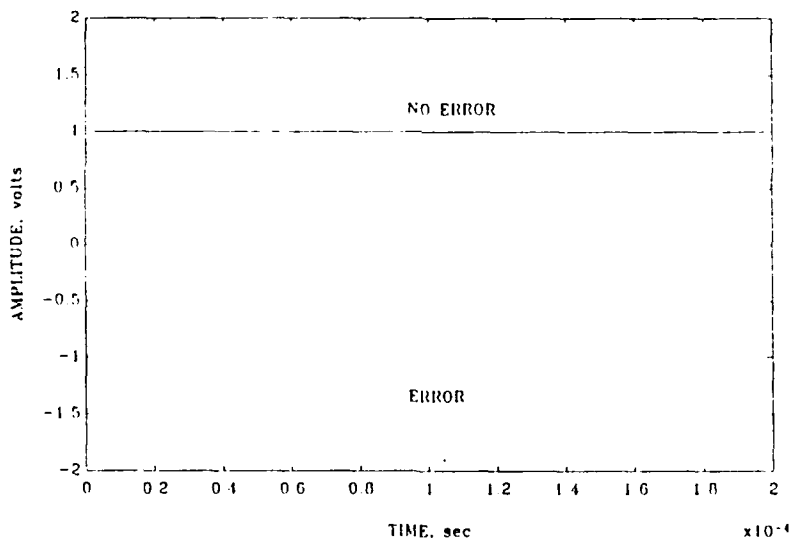


Figure 29 - Error detection output

## 2 - MOVING THE EXCISOR-DETECTOR

One of the objectives was to simulate motion of the detector array to study the effects of the notch passing over the interference signal. For this situation the program was provided with a loop that

simulated this movement. On the following figures the filtering effect can be seen. As the interference passes through the notch (60 KHz wide and 20 dB depth), different attenuation effects take place.

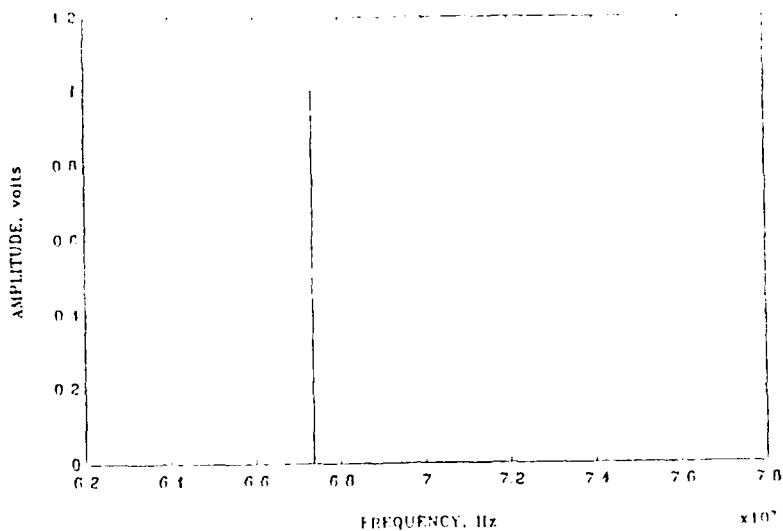


Figure 30 - Test signal spectrum (notch at 67.35 MHz)

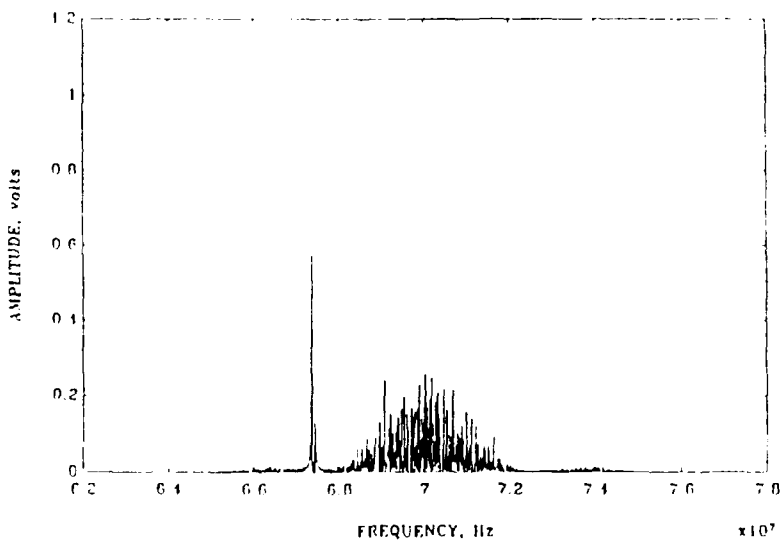


Figure 31 - Test signal spectrum (notch at 67.38 MHz)

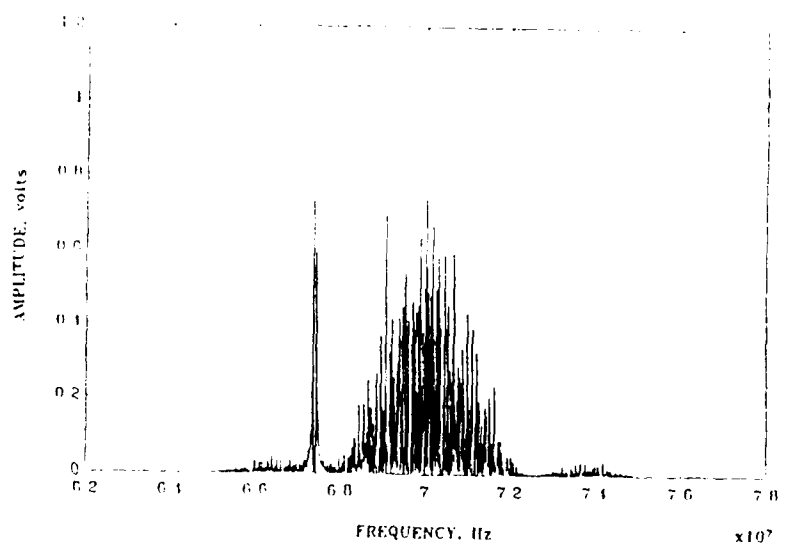


Figure 32 - Test signal spectrum (notch at 67.39 MHz)

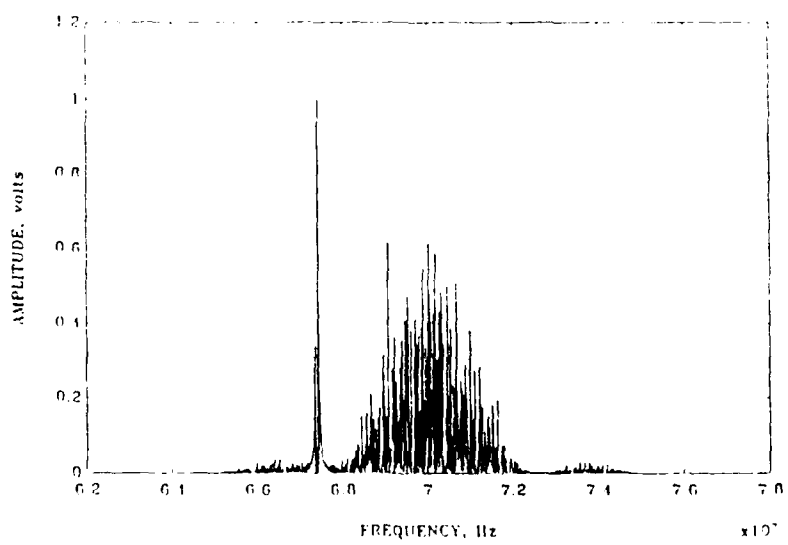


Figure 33 - Test signal spectrum (notch at 67.40 MHz)

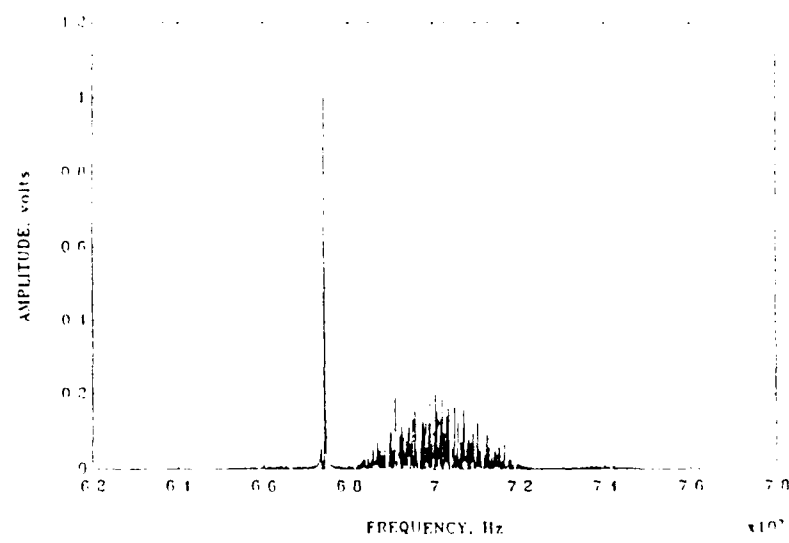


Figure 34 - Test signal spectrum (notch at 67.41 MHz)

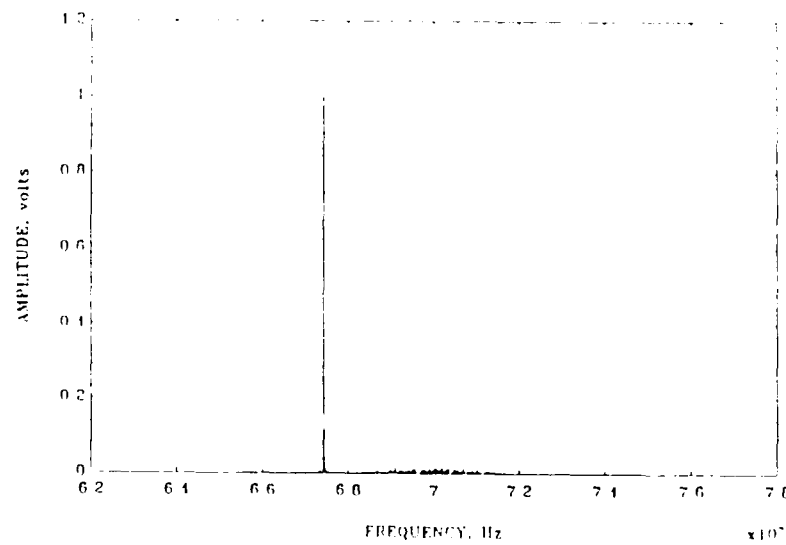


Figure 35 - Test signal spectrum (notch at 67.42 MHz)

As we can see in Figures 30 to 35, a good filtering effect is obtained using a relatively narrow notch with an reasonable attenuation. The interference signal that initially dominates the spectrum was progressively attenuated as the notch was moved over it (see Figure 32).

## VI. CONCLUSIONS AND RECOMMENDATIONS

This thesis has presented the basic principles, characteristics and potential capabilities of optical excisors. The program developed using MATLAB386 provides a consistent tool to aid in the study of acousto-optic spectrum analyzer and excision techniques.

Processing broadband signals requires the removal of strong, narrowband interfering signals. Narrowband interference has been eliminated using a Bragg cell receiver with an excisor-detector at the frequency plane. Moving the excisor-detector by optical and mechanical means made it possible to place a notch with a given characteristic over the narrowband interference signal. The temporal characteristics of the broadband signal are recovered by imaging the filtered light distribution and a reference beam onto a photodetector array to allow coherent detection.

All the results produced with the program during different tests agreed with the values obtained from available references.

Areas for potential use of the program developed are the following:

1. Evaluation of the excision effect varying the notch width and depth using the bit error rate as an indicator of its effectiveness.
2. Testing different input signals and narrowband interference signals.

## APPENDIX A - NOTATION USED IN THE PROGRAM

The notation used consistently throughout this thesis is summarized for the mayor abbreviations and symbols.

a =	Total time
A =	Binary random voltage (Vector)
Ac =	Signal amplitude
b =	Number of binary data
B =	Integrator Output (Vector)
c =	Increment (PRNG)
delta =	Frequency interval
DET =	Coherent detection (Vector)
f =	Frequency axis (Vector)
fc =	Carrier frequency
fi =	Interference central frequency
F =	Channel (Vector)
Fdb =	Detector array filter signal in db (Vector)
FIL =	Detector array filter signal (Vector)
G =	PSD of a BPSK signal theoretical norm.(Vector)
G1 =	PSD of BPSK signal theoretical in dB (Vector)
H =	Recovered signal mapped into binary data (Vector)
I =	Number of loops in the program
k =	Generic counter
m =	Number of samples per bit time (Tb)
mo =	Modulus (PRNG)
n =	Total number of elements in a vector
O =	Right half of a notch (Vector)
Psf1 =	PSD of filtered signal normalized (Vector)
Pss1 =	PSD of signal plus interference normalized (Vector)
PSS =	PSD of signal plus interference in dB (Vector)
PS2 =	PSD of signal without interference normalized (Vec.)

PSS1 = PSD of signal without interference in dB (Vector)  
Q = Left half of a notch (Vector)  
rs = Recovered signal in time domain (Vector)  
RN = Random number (0 - 1)  
s = BPSK signal (Vector)  
sa = Integrator and dump  
si = Interference signal (Vector)  
sd = Signal (BPSK) plus interference (Vector)  
seed = Seed for the pseudorandom number generator  
S = FFT of BPSK signal without interference (Vector)  
SD = FFT of BPSK signal plus Interference (Vector)  
SF = Signal filtered (Vector)  
t = Time axis (Vector)  
u = Generic counter  
zi = Remainder after division (PRNG)

## APPENDIX B - COMPUTER PROGRAM

The following are the different blocks that using MATLAB386 as a master program make possible to perform the simulation and evaluate the results. The titles of each block in bold typeface are not part of the program.

### **BLOCK Input initial Data (INP\_B.m)**

```
echo on
clc
% THIS IS A PROGRAM DEVELOPED IN ORDER TO EVALUATE
% THE FILTERING CAPABILITY OF A NOTCH PRODUCED BETWEEN
% CHANNELS IN A DETECTOR ARRAY.

% NOW YOU WILL BE REQUESTED TO INTRODUCE SOME PARAMETERS

pause % Strike any key to continue

clc
echo on
% THE CARRIER FREQUENCY MUST BE SELECTED BETWEEN 65 AND 75 MHz
% WE SUGGEST 70 MHz IN ORDER TO WORK IN THE CENTER OF THE
% DETECTOR ARRAY.

echo off
input('Which is the Carrier Frequency (Hz)? ');
fc=ans; % Carrier frequency

clc
echo on
% THE AMPLITUDE OF THE SIGNAL MAY BE VARIED
% WE SUGGEST TO USE 1 volt.

echo off
input('Select the Amplitude of the Signal = ');
Ac=ans; % Signal amplitude

clc
echo on
% THE FREQUENCY OF THE INTERFERENCE SIGNAL MUST BE IN THE
% FREQUENCY RANGE OF THE DETECTOR ARRAY OTHERWISE WILL BE
% AUTOMATICALLY FILTERED (65 TO 75 MHz).
```

```

echo off
input('Select the Interference Frequency (Hz) = ');
fi=ans; % Interference Frequency

clc
echo on
% IN ORDER TO RUN THE PROGRAM AND TO SIMULATE THE MOVEMENT
% OF THE DETECTOR ARRAY YOU HAVE TO SELECT THE STEP IN
% FREQUENCY THAT YOU WANT TO CONSIDER FOR EACH LOOP
% FOR EXAMPLE: YOU WANT TO MOVE THE DETECTOR ARRAY IN
% STEPS OF 10 KHz, INSERT THIS VALUE IN Hz (.10000 )

echo off
input('Select the frequency interval (Hz) = ');
delta=ans; % Frequency Interval

input('How many intervals do you want? ');
I=ans; % Number of loops

clc
echo on
% TO PROVIDE THE PROGRAM WITH ONE ESSENTIAL CHARACTERISTIC
% IN TEST AND EVALUATION (IT MUST BE REPRODUCIBLE) IS NECESSARY %
TO INTRODUCE A SEED FOR THE PSEUDORANDOM NUMBER GENERATOR
(PRNG).

echo off
input('Input a SEED for the Random Number Generator = ');
seed=ans; % SEED for PRNG
echo on

save temp_INPUT fc fi Ac delta I
M_BPSK % Calling the main control block

end

```

### *B, OCK Main Control (M\_BPSK.m)*

```

echo off % Turns program display off
clear % Clears memory
FILTER % Develop filter signal
clear
clc
echo off
load temp_INPUT
for k=0:I % Loop for frequency steps
load temp_INPUT
fc=fc+delta*k % Carrier frequency plus
                % interval
fi=fi+delta*k % Interference frequency
pause(3)

```

```

S_BPSK          % Generate the input signal
clear           % Clears memory
FFT_B           % Develops FFT of input
                % signal
clear           % Clears memory
S_FIL           % Calculate the resulting
                % signal passing through the
                % detector array
clear           % Clears memory
IFFT_B          % Develops the IFFT of the
                % filtered signal
clear           % Clears memory
COD_B           % Coherent detection
clear           % Clears memory
end             % End loop
end             % End of main program
cla             % Clears program from memory

```

### **BLOCK Detector Array Filter Signal (FILTER.m)**

```

load temp_S
axis;
clc

% Is time to create the detector array filter signal

%FIL=[ones(1,32768)];           % Simulates no-filter
Q=[1 1 1 1 1 1 1 1 1 1 1];
%      left 1/2 notch
O=[1 1 1 1 1 1 1 1 1 1 1];
%      right 1/2 notch
F=[Q ones(1,126) O];

FIL=[zeros(1,13028) 0:1:1 ones(1,137) ..
O F F F F F F F F F F .. %
Q ones(1,137) 1:-1:0 zeros(1,..    % Detector array
2808) 0:1:1 ones(1,137) ..        % Filter signal
O F F F F F F F F F F .. %
Q ones(1,137) 1:-1:0 zeros(1,13028)];
pause(3)

clc
% We need to create a frequency axis

f=163.84e6*(0:16383)/32768;      % Frequency axis

clc
% The following is a plot of the detector array
% Filter Signal

axis([65e6 75e6 0 1.2]);

```

```

plot(f,FIL(1:16384))...
title('DETECTOR ARRAY FILTER SIGNAL')...
xlabel('FREQUENCY, Hz')...
ylabel('AMPLITUDE, volts')...
pause(5)

clc
% Now we look at the filter magnitude response

FIL1=FIL+eps;
FdB=10*log10(FIL1);

axis([64e6 76e6 -70 10]);
plot(f,FdB(1:16384))...
title('FILTER MAGNITUDE RESPONSE')...
xlabel('FREQUENCY, Hz')...
ylabel('|H(f)|, dB')...
pause(5)

clc
save temp_F FIL f
end

```

### *BLOCK BPSK Signal Generator (S\_BPSK.m)*

```

echo off
load temp_F
clc
a=0.0002; % Total time
t=0:a/32767.5:a; % Time axis
echo on
clc
% In order to produce a BPSK signal we need to generate
% a binary random voltage with values +1 or -1.

c=16807; % Multiplier
mo=2^31-1; % Modulus
zi=seed; % Remainder after division
n=32768; % Total # of elements in the vector
m=64; % # of samples per bit time
b=512; % # of binary data
A=ones(1,n); % Base vector
p=0;
for k=m:m:n % Loop
    g=rem(c*zi,mo); % Pseudorandom number
    RN=g/mo; % generator

```

```

zi=g;
d=(2*round(RN))-1; % [ +1 or -1]
A(1,(p*m)+1:k)=A(1,(p*m)+1:k)*d;
p=p+1;
end % End of Loop
% Now is time to plot the binary data

axis([0 a -Ac-1 Ac+1]);
plot(t,A);
title('BINARY RANDOM DATA');
xlabel('TIME, sec');
ylabel('AMPLITUDE, volts');
pause

clc
% Next we can form a BPSK Signal with a carrier frequency (fc)

s=Ac*A.*cos(2*pi*fc*t); % BPSK Signal
si=3*Ac*sin(2*pi*t*fi); % Interference
sd=s+si; % BPSK signal plus Interference

clc
% Now we are ready to plot the pulse and the BPSK signal

axis([0 0.00002 -Ac-1 Ac+1]);
plot(t,s(1:32768),t,A(1:32768),'-.');
title('BPSK TEST SIGNAL');
xlabel('TIME,sec');
ylabel('AMPLITUDE, volts');
pause

clg
clc
% Plot the BPSK signal plus interference

axis([0 0.00002 -Ac-1 Ac+1]);
plot(t,td);
title('BPSK SIGNAL PLUS INTERFERENCE');
xlabel('TIME,sec');
ylabel('AMPLITUDE');
pause

clg
clc

save temp_S m t s Ac fc a sd A n b
save temp_SR m t Ac A n b a
end

```

### **BLOCK FFT of BPSK Signal (FFT\_B.m)**

```
echo on
load temp_S
load temp_F

clc
% Now we get the Fourier transform of the input signal (BPSK)

S=fft(s); % FFT BPSK Signal
SD=fft(sd); % FFT BPSK Signal + Interference

clc
% In order to plot the power spectral density of the signal we need to
% make some calculations

Pss=SD.*conj(SD);
Pss1=Pss/max(Pss); % PSD Signal + Interference
PSS=10*log10(Pss1); % PSD in dB

Ps1=S.*conj(S);
Ps2=Ps1/max(Ps1); % PSD Signal without interference
PSS1=10*log10(Ps2); % PSD in dB

clc
% Plot the power spectral density of the BPSK signal
% plus interference

axis([fc-5e6 fc+5e6 -90 0]);
plot(f,PSS(1:16384)),...
title('PSD OF BPSK SIGNAL PLUS INTERFERENCE',...
xlabel('FREQUENCY, Hz',...
ylabel('POWER, dB',...
pause
hold on

clc
% For comparison we calculate the theoretical PSD of a BPSK signal

R=(1/((a/32768)*m));
L=(pi*(f-fc)/R)+eps;
K=(Ac2)/(4*R);
X=(sin(L)./L).^2;
PSD=K*X;
G=PSD./max(PSD);
G1=10*log10(G);

clc
```

```

% Now we can plot the theoretical PSD of the BPSK

plot(f,G1(1:16384))...
meta GPSDB.pause
hold off

clc
clc
% For comparison purpose we plot the BPSK signal calculated
% without interference and the theoretical one.

axis([fc-5e6 fc+5e6 -90 0]);
plot(f,PSS1(1:16384))...
title('BPSK SIGNAL COMPARISON')...
xlabel('FREQUENCY, Hz')...
ylabel('POWER, dB')...
text(0.13,0.85,'.....THEORETICAL (dotted line)'...
text(0.13,0.80,'____ CALCULATED (solid line)'...
pause
hold on
plot(f,G1(1:16384))...
pause
hold off

clc
clc

save temp_FFT SD f FIL Pss1 S fc
end

```

### *BLOCK Signal Filtering on the Detector Array (S\_FIL.m)*

```

echo on
load temp_FFT

clc
% Now is time to pass the BPSK signal through the detector array

SF=SD.*FIL; % Filtering the Signal
Psf=SF.*conj(SF);
Psf1=Psf/max(Psf); % PSD Filtered Signal

clc
% First of all we compare the signal spectrum with the filter due
% to the detector array

axis([fc-6e6 fc+6e6 0 1.2]);
plot(f,Pss1(1:16384),f,FIL(1:16384),':',...
title('FILTER SIGNAL & BPSK SPECTRUM ')...

```

```

xlabel('FREQUENCY, Hz')...
ylabel('AMPLITUDE, volts')...
meta GSFIL,pause

clc
% Now we can plot the signal filtered compared to the original one

axis([fc-6e6 fc+6e6 0 1.2]);
plot(f,Psf1(1:16384),f,Pss1(1:16384),':',...
title('BPSK SPECTRUM COMPARISON',...
 xlabel('FREQUENCY, Hz'),...
 ylabel('AMPLITUDE, volts')...
 pause

clc

save temp_SF SF
delete temp_FFT.mat
end

```

### *BLOCK IFFT Signal Filtered (IFFT\_B.m)*

```

echo on
load temp_SF
load temp_S

clc
% Now we return to the time domain taking the inverse
% Fourier transform of the filtered signal

rs=ifft(SF); % Inverse Fourier transform
t=t'; % Arrange time axis

clc
% We can plot the Recovered Signal in the time domain

axis([0 0.00002 -Ac-1 Ac+1])
plot(t,rs),title('RECOVERED BPSK SIGNAL',...
 xlabel('TIME, sec'),...
 ylabel('AMPLITUDE, volts')...
 pause

clc
% Let's compare with the original signal plotting it

```

```

subplot(211),plot(t,s); title('ORIGINAL BPSK'),...
xlabel('TIME, sec'),ylabel('AMPLITUDE',...
subplot(212),plot(t,rs);title('RECOVERED BPSK SIGNAL'),...
xlabel('TIME, sec'),ylabel('AMPLITUDE',...
pause

clc
clear temp_R rs t s m Ac fc
delete temp_SF.mat
delete temp_S.mat
end

```

### **BLOCK Coherent Detector (COD\_B.m)**

```

echo on
load temp_R
load temp_SR
clc
% Now is time to make a coherent detection. The optimum
% detection consist of product detection with an integrator
% that is turned on at the beginning of each bit period
% and integrates to the end of the period.

DET=rs.*cos(2*pi*fc*t); % Coherent detection
B=ones(1,n); % Base vector

for u=0:m:n-m;
    sa=cumsum(DET(1,(u+1:u+m)));
    B(1,(u+1:u+m))=B(1,(u+1:u+m)).*sa;
    sa=0;
end % Loop
% Integrator
% Dump
% End loop

P=-1;
H=ones(1,n);
for v=0:m:n-m;
    dig=B(1,v+m/2);
    if dig>0
        H(1,(v+1:v+m))=H(1,(v+1:v+m)).*1; % Mapped into a digital
    elseif dig<0 % value
        H(1,(v+1:v+m))=H(1,(v+1:v+m)).*P; % Mapped into a digital
    end % value
end % End conditional
% statement
% End Loop

```

```

E=A.*H;                                % Checking for error

clc
% We look at the output of the integrator

axis([0 a -m-1 m+1]);
plot(t,B),...
title('INTEGRATOR OUTPUT'),...
xlabel('TIME, sec'),...
ylabel('AMPLITUDE, volts'),...
pause

clg
clc
% Comparison of the Random Binary Data and the data
% recovered

axis([0 a -Ac-2 Ac+2]);
subplot(211),plot(t,A); title('ORIGINAL BINARY DATA'),...
xlabel('TIME, sec'),ylabel('AMPLITUDE'),...
subplot(212),plot(t,H);title('RECOVERED BINARY DATA'),...
xlabel('TIME, sec'),ylabel('AMPLITUDE'),...
pause

clg
clc

% In order to determine if an error is present we compare
% the data. If we get all 1, there is "no error"; otherwise a -1
% represents an "error".

axis([0 a -2 2]);
plot(t,E),title('ERROR DETECTION'),...
text(0.5,0.75,'NO ERROR','sc')...
text(0.5,0.25,'ERROR','sc')...
xlabel('TIME, sec'),...
ylabel('AMPLITUDE, volts'),...
pause

clg
clc

delete temp_S.mat
delete temp_R.mat
end

```

## APPENDIX C - INFORMATION ABOUT NOTCHES

In order to help the user in the selection of the interference frequency and evaluate the effect in a particular notch, here is a table showing the position of each notch depending how wide it is in the frequency domain.

Notch #	Notch Center	Notch 10 KHz		Notch 20 KHz	
		Start freq.	End freq.	Start freq.	End freq.
1	65900000	65895000	65905000	65890000	65910000
2	66650000	66645000	66655000	66640000	66660000
3	67400000	67395000	67405000	67390000	67410000
4	68150000	68145000	68155000	68140000	68160000
5	68900000	68895000	68905000	68890000	68910000
6	69650000	69645000	69655000	69640000	69660000
7	70400000	70395000	70405000	70390000	70410000
8	71150000	71145000	71155000	71140000	71160000
9	71900000	71895000	71905000	71890000	71910000
10	72650000	72645000	72655000	72640000	72660000
11	73400000	73395000	73405000	73390000	73410000
12	74150000	74145000	74155000	74140000	74160000

Notch #	Notch Center	Notch 30 KHz		Notch 40 KHz	
		Start freq.	End freq.	Start freq.	End freq.
1	65900000	65885000	65915000	65880000	65920000
2	66650000	66635000	66665000	66630000	66670000
3	67400000	67385000	67415000	67380000	67420000
4	68150000	68135000	68165000	68130000	68170000
5	68900000	68885000	68915000	68880000	68920000
6	69650000	69635000	69665000	69630000	69670000
7	70400000	70385000	70415000	70380000	70420000
8	71150000	71135000	71165000	71130000	71170000
9	71900000	71885000	71915000	71880000	71920000
10	72650000	72635000	72665000	72630000	72670000
11	73400000	73385000	73415000	73380000	73420000
12	74150000	74135000	74165000	74130000	74170000

Notch #	Notch Center	Notch 50 KHz		Notch 60 KHz	
		Start freq.	End freq.	Start freq.	End freq.
1	65900000	65875000	65925000	65870000	65930000
2	66650000	66625000	66675000	66620000	66680000
3	67400000	67375000	67425000	67370000	67430000
4	68150000	68125000	68175000	68120000	68180000
5	68900000	68875000	68925000	68870000	68930000
6	69650000	69625000	69675000	69620000	69680000
7	70400000	70375000	70425000	70370000	70430000
8	71150000	71125000	71175000	71120000	71180000
9	71900000	71875000	71925000	71870000	71930000
10	72650000	72625000	72675000	72620000	72680000
11	73400000	73375000	73425000	73370000	73430000
12	74150000	74125000	74175000	74120000	74180000

Notch #	Notch Center	Notch 70 KHz		Notch 80 KHz	
		Start freq.	End freq.	Start freq.	End freq.
1	65900000	65865000	65935000	65860000	65940000
2	66650000	66615000	66685000	66610000	66690000
3	67400000	67365000	67435000	67360000	67440000
4	68150000	68115000	68185000	68110000	68190000
5	68900000	68865000	68935000	68860000	68940000
6	69650000	69615000	69685000	69610000	69690000
7	70400000	70365000	70435000	70360000	70440000
8	71150000	71115000	71185000	71110000	71190000
9	71900000	71865000	71935000	71860000	71940000
10	72650000	72615000	72685000	72610000	72690000
11	73400000	73365000	73435000	73360000	73440000
12	74150000	74115000	74185000	74110000	74190000

Notch #	Notch Center	Notch 90 KHz		Notch 100 KHz	
		Start freq.	End freq.	Start freq.	End freq.
1	65900000	65855000	65945000	65850000	65950000
2	66650000	66605000	66695000	66600000	66700000
3	67400000	67355000	67445000	67350000	67450000
4	68150000	68105000	68195000	68100000	68200000
5	68900000	68855000	68945000	68850000	68950000
6	69650000	69605000	69695000	69600000	69700000
7	70400000	70355000	70445000	70350000	70450000
8	71150000	71105000	71195000	71100000	71200000
9	71900000	71855000	71945000	71850000	71950000
10	72650000	72605000	72695000	72600000	72700000
11	73400000	73355000	73445000	73350000	73450000
12	74150000	74105000	74195000	74100000	74200000

Notch #	Notch Center	Notch 110 KHz		Notch 120 KHz	
		Start freq.	End freq.	Start freq.	End freq.
1	65900000	65845000	65955000	65840000	65960000
2	66650000	66595000	66705000	66590000	66710000
3	67400000	67345000	67455000	67340000	67460000
4	68150000	68095000	68205000	68090000	68210000
5	68900000	68845000	68955000	68840000	68960000
6	69650000	69595000	69705000	69590000	69710000
7	70400000	70345000	70455000	70340000	70460000
8	71150000	71095000	71205000	71090000	71210000
9	71900000	71845000	71955000	71840000	71960000
10	72650000	72595000	72705000	72590000	72710000
11	73400000	73345000	73455000	73340000	73460000
12	74150000	74095000	74205000	74090000	74210000

To put the correct value in the notch filter that represent a given attenuation in dB, a table with different values of attenuation from 0 to -45 dB is presented.

#### ATTENUATION TABLE

Attenuation (dB)	Number	Attenuation (dB)	Number
0	1.00000	-11	0.07943
-1	0.79432	-12	0.06309
-2	0.63096	-13	0.05119
-3	0.50119	-14	0.03981
-4	0.39811	-15	0.03162
-5	0.31623	-20	0.01000
-6	0.25119	-25	0.00316
-7	0.19953	-30	0.00100
-8	0.15849	-35	0.00032
-9	0.12589	-40	0.00010
-10	0.10000	-45	0.00003

## APPENDIX D - DEFINITIONS

A group of useful definitions related to this work are presented.

**Bragg cell** : The heart of all acousto-optic systems. A thin slab of a transparent crystal (such as tellurium oxide, lithium niobite, or gallium phosphide) with one or more piezoelectric transducers attached. When a microwave signal excites the transducer, it creates an ultrasound wave into the crystal. This wave changes the optical index of refraction at the microwave frequency [Ref. 9].

**Excisor-detector**: An array of photodetectors which is inserted into the frequency plane of an optical spectrum analyzer. The small spaces between detectors are used as spatial light modulators, that produce notches in the frequency response.

**Model** : Mathematical representation of a system or part of a system and/or some portion of its environment. The model is a set of equations which may be solved manually or by means of a computer to determine the behavior of the system under a specific set of conditions or during a series of sets of conditions. Models permit easy modification of the system parameters to determine the effects of such changes on system performance [Ref. 10].

**Simulation** : Simulations include techniques for representing a system or part of a system and/or some portion of its environment (including human interfaces with hardware) through the use of substitutes for all or part of the real hardware, personnel; and environment. Thus simulation covers a more extensive field than modeling, although most models are also simulations [Ref. 10].

## LIST OF REFERENCES

1. Goutzoulis, Anastasios P. and Abramovitz, Irwin J., "Digital Electronics meets its match", *IEEE Spectrum*, pp. 21-25, August 1988.
2. Turpin, Terry M., "Spectrum Analysis Using Optical Processing", *Proceedings of the IEEE*, vol. 69, N° 1, pp. 79-92, January 1981.
3. Berg, Norman J. and Lee, John N., *Acousto-Optic Signal Processing*, Marcel Dekker, Inc., 1983.
4. Little, John; Moler, Cleve; Bangert, Steve and Kleiman, Steve, *MATLAB 386 User's Guide*, The MathWorks, Inc., 1989.
5. Markevitch, Bob V. and Kooij, Theo, "Bragg Signal Processing and Output Devices", *Proceedings of SPIE*, Vol. 352, pp. 17-23, August 1982.
6. Smith, D. E., *Acoustooptic Spectral Excision of Narrowband Interference*, Engineer's Thesis, Naval Postgraduate School, Monterey California, 1980.
7. Couch, Leon W., *Digital and Analog Communications Systems*, Macmillan Publishing Company, 1987.
8. LCDR. Walsh , *Notes OS-3303 Computer Simulation*, Naval Postgraduate School, Monterey, California, 1988 (unpublished).
9. Korpel, Adrianus, "Acousto-optics - A Review of Fundamentals", *Proceedings of the IEEE*, vol. 69, N° 1, pp. 48-53, January 1981.
10. Stevens, Roger T., *Operational Test and Evaluation: A System Engineering Process*, Robert E. Krieger Publishing Co., 1986.
11. Ericson, Jerry L., *Linear Acousto-optic Filtering with Heterodyne and Frequency-plane Control*, Ph.D. Dissertation, Standford University, University Microfilms International, June 1981.

12. Oakley, William S., "Acousto-optical Processing Opens New Vistas in Surveillance and Warning Receivers", *Defense Electronics*, pp. 91-101, October 1979.
13. Hecht, D. L. and Chang I. C., "Characteristic of Acousto-optic Devices for Signal Processors", *Optical Engineering*, vol. 21, Nº 1, pp. 76-81, January/February 1982.

## INITIAL DISTRIBUTION LIST

	Nº of Copies
1. Defense Technical Information Center Cameron Station Alexandria, Virginia 22304-6145	2
2. Library, Code 0142 Naval Postgraduate School Monterey, California 93943-5002	2
3. Professor John P. Powers, Code 62 Department of Electrical Engineering Naval Postgraduate School Monterey, California 93943	3
4. Professor Glen A. Myers, Code 62 Mv Department of Electrical Engineering Naval Postgraduate School Monterey, California 93943	1
5. Professor David D. Cleary, Code 61 CL Department of Physics Naval Postgraduate School Monterey, California 93934	1
6. Commander Space and Naval Warfare Systems Command (Attn: PMW 144-2, CDR Frentzel) Washington DC 20363-5103	1
7. Comando de Operaciones Navales Edificio Libertad Comodoro Py 2055 Buenos Aires (1104) República Argentina	2

8.	Dirección de Instrucción Naval Edificio Libertad Comodoro Py 2055 Buenos Aires (1104) República Argentina	2
9.	Comisión Naval Argentina en los E.E.U.U. Sr. Jefe de la Comisión Naval Argentina 630 Indiana Ave. NW, Washington, DC, 20004	1
10.	Comando de Flota de Mar Edificio Libertad Comodoro Py 2055 Buenos Aires (1104) República Argentina	1
11.	Comando de Aviación Naval Edificio Libertad Comodoro Py 2055 Buenos Aires (1104) República Argentina	1
12.	Escuela de Oficiales de la Armada Edificio Libertad Comodoro Py 2055 Buenos Aires (1104) República Argentina	1
13.	LT Daniel A. Marinsalta Edificio Libertad Comodoro Py 2055 Buenos Aires (1104) República Argentina	2